Article

Current Biology

Functions of Opsins in *Drosophila* Taste

Graphical Abstract

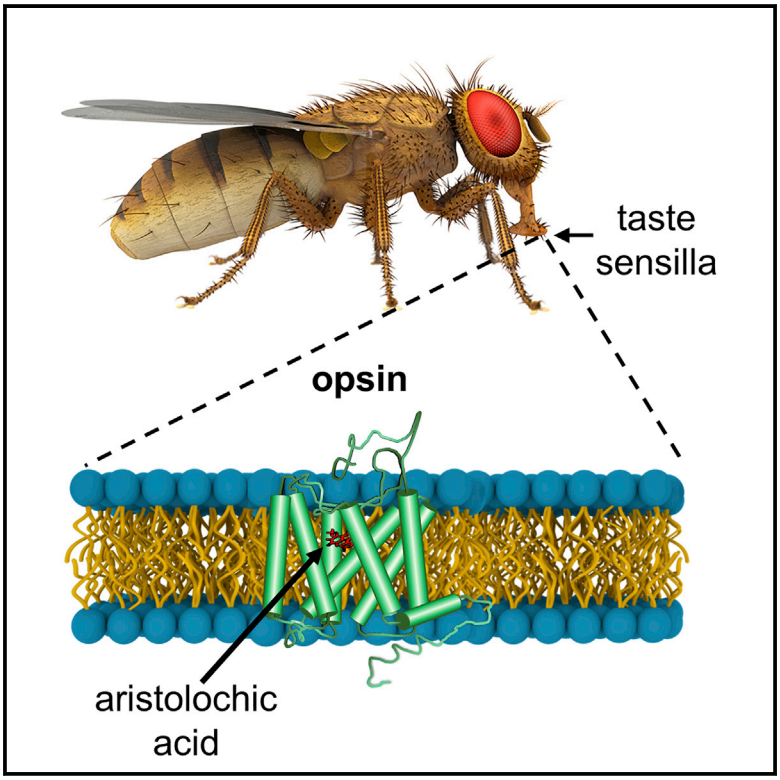

Authors

Nicole Y. Leung, Dhananjay P. Thakur, Adishthi S. Gurav, Sang Hoon Kim, Antonella Di Pizio, Masha Y. Niv, Craig Montell

Correspondence

cmontell@ucsb.edu

In Brief

Rhodopsins sense light and consist of an opsin and retinal. Using flies, Leung et al. find that opsins detect bitter compounds and are needed for taste. The opsins promote sensing low amounts of chemicals via a signaling cascade that includes TRPA1. This function is independent of light and retinal and reveals a role for opsins as chemosensors.

Highlights

- Opsins are needed for bitter taste in *Drosophila*
- Opsins are directly activated by bitter tastants
- Role for opsins in taste is independent of light and retinal
- Opsins sense low levels of tastants via a signaling cascade that includes TRPA1

Leung et al., 2020, Current Biology *30*, 1367–1379
April 20, 2020
https://doi.org/10.1016/j.cub.2020.01.068

CellPress

Current Biology
Article

CellPress

Functions of Opsins in *Drosophila* Taste

Nicole Y. Leung,[1,2] Dhananjay P. Thakur,[1,2] Adishthi S. Gurav,[1,2] Sang Hoon Kim,[3] Antonella Di Pizio,[4,5,6] Masha Y. Niv,[4,5] and Craig Montell[1,2,7,*]

[1]Neuroscience Research Institute, University of California, Santa Barbara, CA 93106, USA
[2]Department of Molecular, Cellular and Developmental Biology, University of California, Santa Barbara, CA 93106, USA
[3]Department of Biological Chemistry, The Johns Hopkins University School of Medicine, Baltimore, MD 21205, USA
[4]Institute of Biochemistry, Food Science and Nutrition, The Robert H. Smith Faculty of Agriculture, Food and Environment, The Hebrew University of Jerusalem, 76100 Rehovot, Israel
[5]The Fritz Haber Center for Molecular Dynamics, The Hebrew University of Jerusalem, 91904 Jerusalem, Israel
[6]Leibniz-Institute for Food Systems Biology at the Technical University of Munich, 85354 Freising, Germany
[7]Lead Contact
*Correspondence: cmontell@ucsb.edu
https://doi.org/10.1016/j.cub.2020.01.068

SUMMARY

Rhodopsin is a light receptor comprised of an opsin protein and a light-sensitive retinal chromophore. Despite more than a century of scrutiny, there is no evidence that opsins function in chemosensation. Here, we demonstrate that three *Drosophila* opsins, Rh1, Rh4, and Rh7, are needed in gustatory receptor neurons to sense a plant-derived bitter compound, aristolochic acid (ARI). The gustatory requirements for these opsins are light-independent and do not require retinal. The opsins enabled flies to detect lower concentrations of aristolochic acid by initiating an amplification cascade that includes a G-protein, phospholipase Cβ, and the TRP channel, TRPA1. In contrast, responses to higher levels of the bitter compound were mediated through direct activation of TRPA1. Our study reveals roles for opsins in chemosensation and raise questions concerning the original roles for these classical G-protein-coupled receptors.

INTRODUCTION

Animals rely heavily on contact chemosensation to evaluate food quality, such as flavor and nutritional value. The chemical perception of food is initiated through the binding of tastants to receptor proteins that are expressed in specialized peripheral gustatory receptor cells [reviewed in 1]. The information is then delivered to the central nervous system, ultimately contributing to the decision to ingest or reject the food. Thus, peripheral taste coding is essential for an animal to avoid consuming harmful substances, which are often bitter.

To date, all taste receptors identified in insects are known or putative ion channels [reviewed in 1]. The employment of ligand-gated cation channels in sensing attractive and aversive compounds in insects differs greatly from mammalian sweet, bitter, and umami tastes, which function through signaling cascades that are initiated by G-protein-coupled receptors (GPCRs). Once activated, mammalian taste receptors subsequently couple to a phospholipase C (PLC)-dependent signaling cascade, which culminates with activation of the transient receptor potential (TRP) channels, TRPM4 and TRPM5 [2–5]. A limitation of ionotropic receptors that are used in fly taste is that they do not allow for signal amplification, which would enable detection of chemicals at lower amounts than would otherwise be possible. A hint that a mammalian-like taste transduction cascade exists in insects is the finding that gustatory detection of the plant-derived bitter compound aristolochic acid (ARI) depends on PLC-β and TRPA1 [6].

In this study, we found that three *Drosophila* opsins, Rh1, Rh4, and Rh7, are needed for sensation of ARI but only at the lower concentrations tested. Although the lower amounts of ARI were detected through an opsin-initiated signaling cascade coupled to G_q, PLC-β, and TRPA1, flies responded to the higher concentrations of the same chemical through direct activation of TRPA1. These findings provide the first demonstration that opsins function in chemosensation since their discovery in the 19th century [7–10]. Given the recent findings that rhodopsins contribute to thermosensation, hearing, and proprioception [11–14], we propose that rhodopsins represent a class of polymodal sensory receptor with roles potentially as diverse as TRP channels.

RESULTS

Requirements of Rh1, Rh4, and Rh7 for Avoiding Aristolochic Acid

The requirement for PLC-β and TRPA1 for sensing ARI [6] raised the possibility that one or more GPCRs are the receptors that initiate the signaling cascade coupled to these proteins. We tested whether opsins are the GPCRs, given that their activities are linked to PLC-β. We allowed flies to choose between 2 mM sucrose alone versus 2 mM sucrose plus ARI, mixed with red or blue food dye. We inspected the color of the abdomens and calculated a preference index (PI). A PI = 1.0 or −1.0 results from complete preference for one or the other food, whereas a PI = 0 indicates indifference to the two options. The red food coloring at 0.2 mg/mL or blue coloring at 0.08 mg/mL did not cause bias when combined with sucrose only (Figure S1A). Moreover, the flies displayed similar repulsion to 1 mM ARI regardless of the dye color (Figure S1B) (PI = 0.58 ± 0.03 and 0.52 ± 0.03).

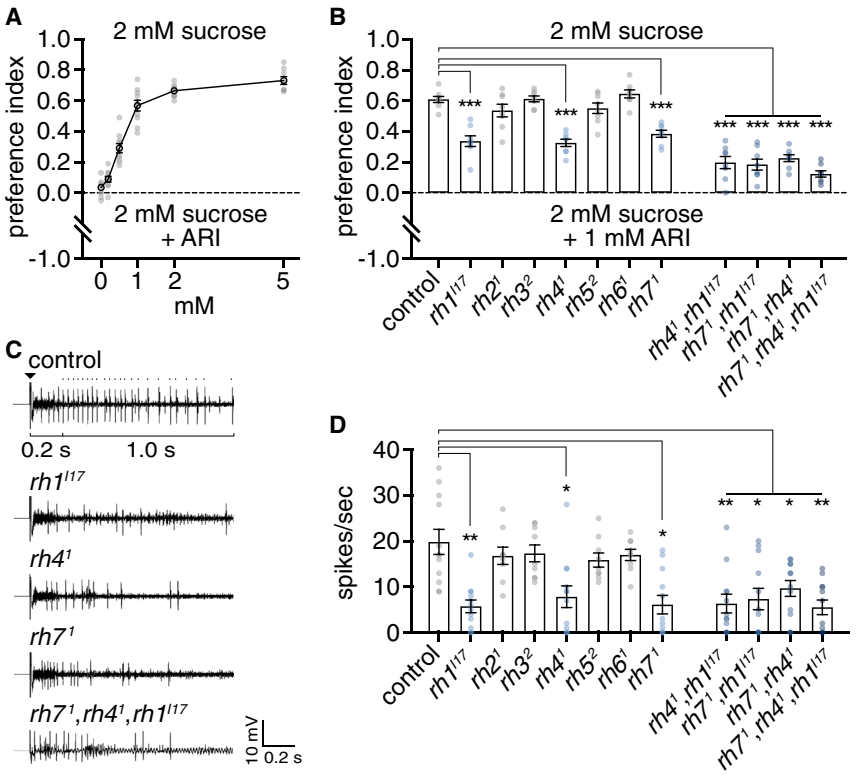

Figure 1. Fly Avoidance of Aristolochic Acid Requires Rh1, Rh4, and Rh7

(A) Two-way choice feeding assays testing preferences of control (w^{1118}) flies for 2 mM sucrose versus 2 mM sucrose plus the indicated concentrations of ARI. n = 8–10 for each concentration. Means ± SEMs. See also Figures S1A and S1B.

(B) Two-way choice feeding assays testing preferences of *opsin* mutants for 2 mM sucrose versus 2 mM sucrose plus 1 mM ARI. n = 8 per genotype. Means ± SEMs. Statistics performed using one-way ANOVA with Tukey's multiple comparisons test. See also Figure S1D and Table S1.

(C) Representative tip recording traces by stimulating S6 sensilla of the indicated flies with 1 mM ARI (arrowhead indicates contact of the sensillum with the electrode). The larger amplitudes spikes are ARI-induced action potentials. Dots above the control trace denote the counted spikes between 200–1,200 ms following contact.

(D) Quantification of tip recording action potentials between 200–1,200 ms following application of 1 mM ARI. n = 9–12 per genotype. Means ± SEMs. Statistics performed using Kruskal-Wallis test with Dunn's multiple comparisons test. See also Figures S1E, S1G, and S1H and Table S1.

*p < 0.05, **p < 0.01, and ***p < 0.001.

The aversion to ARI displayed the steepest dose dependence at concentrations ≤ 1.0 mM (Figure 1A).

We screened all seven *opsin* mutants for defects in avoiding 1 mM ARI. Although mutations disrupting four of the opsins had no effect on control flies, we found that significant impairments in avoidance were caused by null mutations affecting any of three *opsin* genes: *rh1* (also known as *ninaE*), *rh4*, and *rh7* (Figure 1B) (PI = 0.34 ± 0.03, 0.33 ± 0.02, and 0.39 ± 0.02, respectively). In contrast, the GR66a and GR33a gustatory receptors, which function in the taste avoidance of many aversive compounds [15–18], were dispensable for sensing ARI (Figure S1C).

Each of the three *opsin* mutations also resulted in defects in avoiding ARI when placed *in trans* with deficiencies that removed the corresponding genes ($rh1^{I17}$/Df, $rh4^{1}$/Df, and $rh7^{1}$/Df) (Figure S1D). The distaste for 1 mM ARI exhibited by the double mutants ($rh4^{1}$,$rh1^{I17}$, $rh7^{1}$,$rh1^{I17}$, and $rh7^{1}$,$rh4^{1}$) and triple mutants ($rh7^{1}$,$rh4^{1}$,$rh1^{I17}$) was greatly reduced compared with the control (Figure 1B) (PI = 0.20 ± 0.04, 0.18 ± 0.04, 0.23 ± 0.02, and 0.12 ± 0.02, respectively). The differences between single and double mutants and single and triple mutants were mostly significant, although the slightly lower preference index exhibited by the triple mutant than the double mutants was not significant (Table S1).

Opsins Function in Bitter-Responsive GRNs for Sensing Aristolochic Acid

We performed extracellular electrophysiological recordings (tip recordings) to examine whether Rh1, Rh4, and Rh7 function in gustatory receptor neurons (GRNs). Each bilaterally symmetrical labellum contains ~31 bristles (sensilla), each of which houses two or four GRNs [reviewed in 1]. Taste sensilla are categorized into three classes, including small (S-type) sensilla, most of which respond to aversive tastants. We recorded from S6 sensilla because they contain GRNs that display the highest frequencies of aristolochic-acid-induced action potentials [6, 19]. Upon stimulation with 1 mM ARI, control flies exhibited 19.8 ± 2.7 spikes per second (Figures 1C and 1D). We found that flies lacking Rh1, Rh4, or Rh7 showed large decreases in neuronal firing (Figures 1C and 1D) (5.8 ± 1.4, 7.8 ± 2.4, and 6.1 ± 2.0 spikes per second, respectively). We observed similar reductions in action potentials when we placed each mutation *in trans* with the corresponding deficiencies (Figures S1E and S1G). The single, double, and triple mutants exhibited similar decreases in action potential firing in response to 1 mM ARI (Figures 1C, 1D, and S1H). This differs from the significantly greater deficits in behavior between the single and double mutants (Table S1). However, it is difficult to precisely correlate concentrations of tastants used for behavior and tip recordings given that the latter involves placing chemicals in a recording electrode, which directly contacts the endolymph surrounding the dendrites. Therefore, we performed tip recordings using slightly lower amounts of ARI (0.5 mM) and found that the triple mutant produced fewer action potentials than the single mutants (Figure S1F). Nevertheless, because the action potential frequencies were already low with the single mutants, the further reduction in the triple mutant was not statistically significant.

Only one bitter-responsive GRN is housed in a sensillum, suggesting that the opsins function in the same GRNs. To address this possibility, we first determined whether all of the opsins function in bitter-responsive GRNs. We tested whether

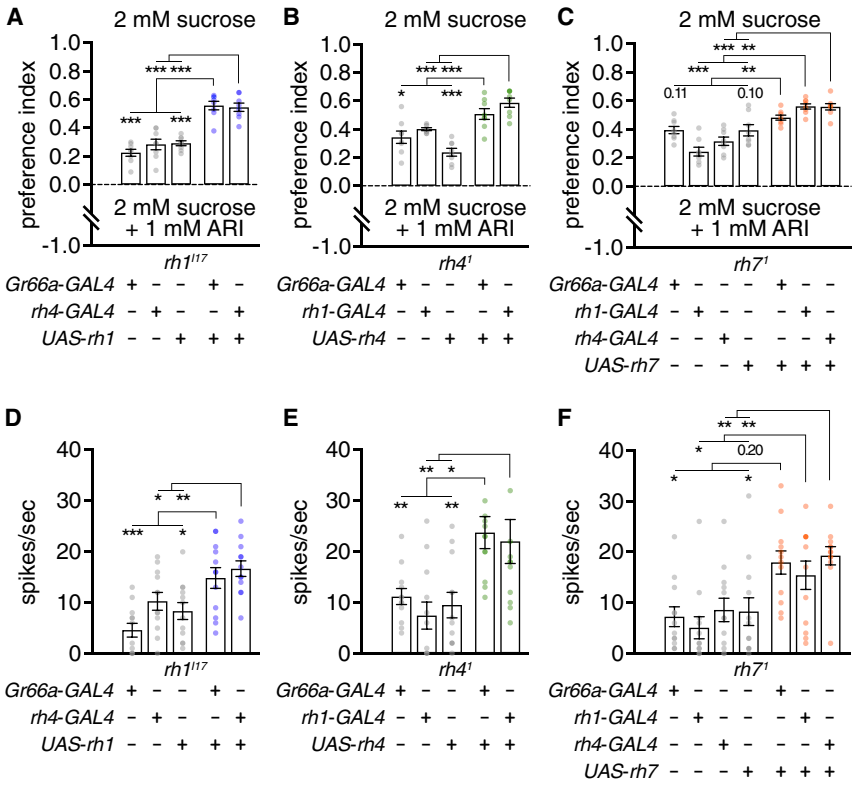

Figure 2. Requirements for Opsins in GRNs for Detecting Aristolochic Acid

(A–C) Two-way choice feeding assays testing the preferences for 2 mM sucrose versus 2 mM sucrose plus 1 mM ARI. n = 8 per genotype. Means ± SEMs. Statistics performed using one-way ANOVA with Tukey's multiple comparisons test.

(D–F) Quantification of tip recording action potentials of the indicated flies between 200–1,200 ms following application of 1 mM ARI. n = 12 per genotype. Means ± SEMs. Statistics performed using the Kruskal-Wallis test with Dunn's multiple comparisons test. See also Figures S2A–S2C.

(A and D) Rescue of the $rh1^{I17}$ mutant (A) behavioral and (D) electrophysiological phenotypes by expressing *UAS-rh1* using the indicated *GAL4*.

(B and E) Rescue of $rh4^{1}$ mutant (B) behavioral and (E) electrophysiological phenotypes by expressing *UAS-rh4* using the indicated *GAL4*.

(C and F) Rescue of $rh7^{1}$ mutant (C) behavioral and (F) electrophysiological phenotypes by expressing *UAS-rh7* using the indicated *GAL4*.

*p < 0.05, **p < 0.01, and ***p < 0.001.

we could rescue the $rh1^{I17}$, $rh4^{1}$, and $rh7^{1}$ mutant phenotypes by using the corresponding rescue transgenes driven by *Gr66a-GAL4*, which directs expression in bitter-responsive GRNs [20]. We found that the behavioral (Figures 2A–2C) and electrophysiological impairments (Figures 2D, 2F, and S2A–S2C) in responding to ARI were all rescued, indicating that the opsins function in bitter-responsive GRNs. To test whether the opsins function in the same GRNs, we used the *rh1-GAL4* and *rh4-GAL4* to drive expression of the various *UAS-opsin* transgenes, in each of the three mutant backgrounds. The *rh1-GAL4* and *rh4-GAL4* were both effective for this purpose because they rescued the mutant phenotypes exhibited by the $rh1^{I17}$ and $rh4^{1}$ mutants when we combined them with *UAS-rh1* and *UAS-rh4*, respectively (Figures S2D and S2F). The *rh1-GAL4* and *rh4-GAL4* also rescued each of the mutant phenotypes when we used them to drive the corresponding rescue transgenes (Figures 2A–2F and S2A–S2C), indicating that the opsins function in the same GRNs.

Gustatory Roles of Opsins Do Not Need the Chromophore

Rh1, Rh4, and Rh7 are light sensors [21, 22], raising the question as to whether ARI repulsion is affected by light. The two-way choice feeding assays were performed in the dark, suggesting that the behavior is not light dependent. To test whether light affects ARI repulsion, we compared the behavior in the dark and light, and found that avoidance was not significantly different (Figure 3A). Moreover, bright light did not significantly affect ARI avoidance in flies expressing *opsin* transgenes under control of the *Gr66a-GAL4* driver (Figure S3A).

In fly photoreceptor cells, the chromophore (3-hydroxy-11-*cis*-retinal) serves as a light sensor and as a molecular chaperone, which is needed for rhodopsin to exit the endoplasmic reticulum [23, 24]. Therefore, even though the roles for the opsins in sensing ARI were light-independent, we could not exclude that the retinal is required for chemosensation. To test this question, we eliminated a scavenger receptor, NINAD, which promotes the uptake of carotenoids in the midgut [25–27]. However, $ninaD^{1}$ mutant flies still produced a substantial light response, as assessed by performing electroretinogram recordings (Figures 3B and 3C). We reduced chromophore amounts further by maintaining $ninaD^{1}$ flies on carotenoid-free food and did so for multiple generations to minimize maternal transfer of retinoids. Although there was virtually no light response after one or two generations on this diet (Figures S3B and S3C), we continued to maintain $ninaD^{1}$ flies on carotenoid-free food for three generations ($ninaD^{1}$ F3). We found that the $ninaD^{1}$ F3 flies, which were unresponsive to light (Figure 3D), showed normal aversion to 1 mM ARI (Figure 3E) and a normal frequency of ARI-induced action potentials compared with controls maintained on standard food (Figures 3F and 3G). These results indicate that the chromophore is dispensable for taste.

We further tested whether the retinal is dispensable for sensing ARI by introducing an amino acid substitution in Rh1 that prevents it from binding the chromophore. Retinal forms a covalent linkage with a lysine in the seventh transmembrane domain of opsins [28] (residue 319 in Rh1) [29, 30]. Therefore, we changed lysine 319 to an arginine and expressed the $UAS\text{-}rh1^{K319R}$ transgene in a $rh1^{I17}$ null background by using the *Gr66a-GAL4*. We found that $rh1^{K319R}$ flies showed normal ARI repulsion (Figure 3H) and normal aristolochic-acid-induced action potentials (Figures 3I and 3J). Altogether, these data demonstrate that the Rh1 apoprotein is sufficient for functioning in the gustatory response.

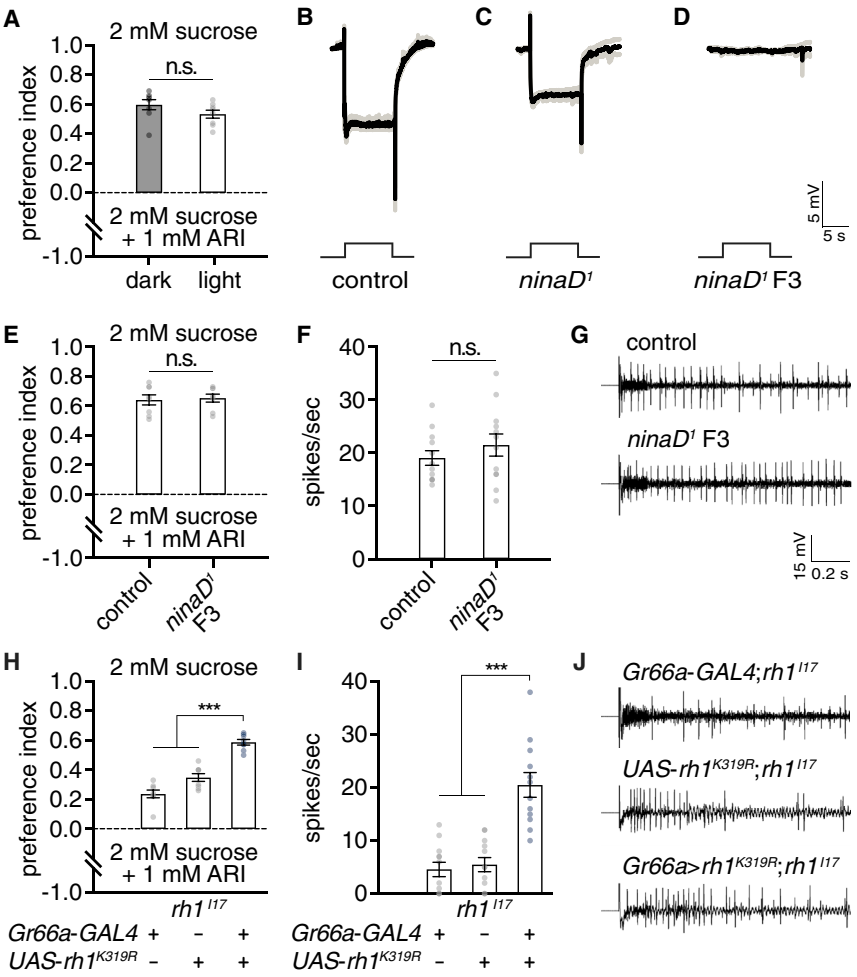

Figure 3. Chromophore Is Dispensable for Opsin-Mediated Chemosensation

(A) Light does not significantly affect ARI repulsion. Two-way choice feeding assays testing the preferences of control (w^{1118}) flies for 2 mM sucrose versus 2 mM sucrose plus 1 mM ARI in the dark (gray) versus light (white). n = 8 per condition. Means ± SEMs. Statistics performed by using the unpaired Student's t test.

(B–D) Electroretinogram recordings of (B) control and (C) *ninaD*^{1} flies reared on standard food and (D) *ninaD*^{1} flies reared on carotenoid-deficient food for three generations (F3). The flies were exposed to a 10 s light pulse. The black trace represents the mean and the gray traces represent ± SEMs. n = 4 per condition. See also Figures S3B and S3C.

(E) Two-way choice feeding assays testing the preferences of control and *ninaD*^{1} F3 flies for 2 mM sucrose versus 2 mM sucrose plus 1 mM ARI. n = 8 per genotype. Means ± SEMs. Statistics were performed by using the unpaired Student's t test.

(F) Quantification of tip recording action potentials of control and *ninaD*^{1} F3 flies between 200–1,200 ms after application of 1 mM ARI. n = 12 per genotype. Means ± SEMs. Statistics were performed by using the unpaired Student's t test.

(G) Representative tip recording traces (Figure 3F) by stimulating S6 sensilla with 1 mM ARI.

(H and I) Rescue of the *rh1*^{I17} phenotype by expressing *UAS-rh1*^{K319R} via the *Gr66a-GAL4*. Shown in (H) are two-way choice feeding assays testing the preferences for 2 mM sucrose versus 2 mM sucrose plus 1 mM ARI. n = 8 per genotype. Shown in (I) is a quantification of tip recording action potentials between 200–1,200 ms after application of 1 mM ARI. n = 12 per genotype. Means ± SEMs. Statistics were performed by using one-way ANOVA with Tukey's multiple comparisons test.

(J) Representative tip recording traces (Figure 3I) by stimulating S6 sensilla with 1 mM ARI.

***$p < 0.001$.

Requirement for Opsins in Adults for Gustatory Avoidance of Aristolochic Acid

Rhodopsins are expressed at extremely high amounts in photoreceptor cells for efficient photon capture. However, the contributions of *rh1*, *rh4*, and *rh7* to taste are not affected by light, suggesting that they might be expressed at low amounts in GRNs, potentially to avoid photon capture. Indeed, we were unable to detect opsin proteins in GRNs by using Rh1, Rh4, or Rh7 antibodies, even after tyramide amplification. Therefore, we employed RT-PCR as well as quantitative RT-PCR (RT-qPCR) to assay for *opsin* RNA expression in the labellum. Using these approaches, we detected *rh1*, *rh4*, and *rh7* transcripts in the labellum of control flies (RT-PCR, Figures 4A–4C; RT-qPCR, Figures 4D–4I). The signals were specific given that they were absent in the null mutants (Figures 4A–4I). As described above, light did not interfere with ARI avoidance even when we expressed the opsins in bitter GRNs by using the *Gr66a-GAL4* driver (Figure S3A). However, GRNs do not include microvilli, which in fly photoreceptor cells enable rhodopsins to accumulate to the high amounts necessary for efficient photon capture. Thus, the lack of light sensitivity might be because of the combination of low expression of the opsins and minimal retinal in the GRNs.

The question arises as to whether the opsins function in bitter taste in the adult, or whether the defects in ARI sensation in the opsin mutants reflect roles during development. Therefore, we conducted tissue-specific, temperature-controlled RNAi-mediated knockdown of *rh1*, *rh4*, and *rh7* by using the *Gr66a-GAL4* driver, which is expressed ubiquitously in bitter GRNs. To temporally control the activity of the GAL4 transcription factor, we employed a transgene encoding a temperature-sensitive GAL4 repressor (GAL80^{ts}), which is expressed under the control of the *tubulin* promoter (*tubulin-GAL80*^{ts}). GAL80^{ts} is functional at 18°C and inhibits GAL4 activity, thereby preventing RNAi-mediated knockdown at 18°C. At 29°C, the GAL80^{ts} is inactive. Consequently, RNAi knockdown occurs at 29°C. To induce RNAi knockdown only in the adults, we raised flies at 18°C and then shifted the animals to 29°C upon eclosion. We then performed two-way choice feeding assays and tip recordings on 5-day-old flies.

We found that knockdown of *rh1*, *rh4*, and *rh7* in the adult stage resulted in defects in the gustatory sensation of ARI. These include impairments in behavioral avoidance of ARI and reductions in action potentials (18° → 29°) (Figures 4J and 4K). This was not due to effects of temperature alone because there were no differences in aristolochic-acid-induced avoidance or

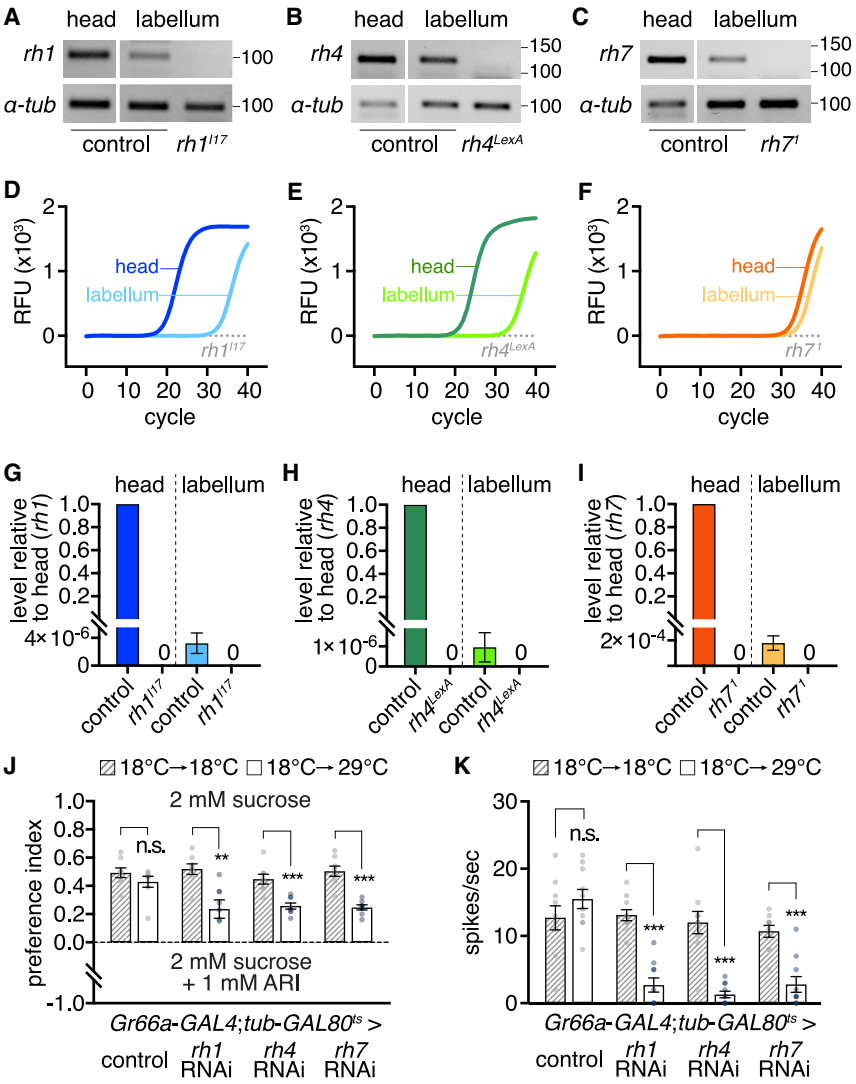

Figure 4. Expression of *Opsins* in the Labellum

(A–C) RT-PCR products of (A) *rh1*, (B) *rh4*, and (C) *rh7* using complementary DNA (cDNA) from control (w^{1118}) heads without labella, control labella, or mutant labella. α-*tubulin* (α-*tub*) served as the internal control.

(D–F) Quantitative RT-PCR amplification curves using cDNA from control heads without labella, control labella, or mutant labella. The data are the mean of 3 independent experiments. In (D), *rh1* transcripts in control heads are in blue, control labella in light blue, and $rh1^{l17}$ labella in gray. In (E), *rh4* transcripts in control heads are shown in green, control labella in light green, and $rh4^{LexA}$ labella in gray. In (F) *rh7* transcripts in control heads are in orange, control labella in light orange, and $rh7^{1}$ labella in gray. Abbreviation is as follows: RFU, relative fluorescent units.

(G–I) *opsin* transcript levels relative to the control head obtained from quantitative RT-PCR reactions using cDNA from control heads without labella, control labella, or mutant labella. In (G) *rh1* transcripts in control heads are in blue, control labella in light blue, and $rh1^{l17}$ labella in gray. In (H) *rh4* transcripts in control heads are in green, control labella in light green, and $rh4^{LexA}$ labella in gray. In (I) *rh7* transcripts in control heads are in orange, control labella in light orange, and $rh7^{1}$ labella in gray. Means ± SEMs from ≥ 3 independent experiments. See also Figure S4M.

(J and K) Effects of RNAi knockdown of *rh1*, *rh4*, or *rh7*, specifically in adult flies, on the responses to ARI. The *UAS-RNAi* lines were expressed using the *Gr66a-GAL4*. Temperature control of GAL4 activity was mediated by the temperature-sensitive GAL4 inhibitor, $GAL80^{ts}$ (*tub-GAL80*^{ts}). $GAL80^{ts}$ is active and inactive at 18° and 29°C, respectively. Flies were either (1) raised at 18°C and maintained at 18°C after eclosion (shown in gray; 18°C→18°C; no RNAi), or (2) raised at 18°C and transferred to 29°C upon eclosion (shown in white; 18°C→29°C; RNAi in adults only).

(J) Two-way choice feeding assays testing preferences for 2 mM sucrose versus 2 mM sucrose plus 1 mM ARI. n = 8 per genotype. Means ± SEMs. Statistics were performed by using the unpaired Student's t test.

(K) Quantification of tip recording action potentials between 200–1,200 ms after application of 1 mM ARI. n = 8 per genotype. Means ± SEMs. Statistics were performed by using the unpaired Student's t test.

**p < 0.01 and ***p < 0.001.

action potentials at 18° and 29°C in the absence of an RNAi transgene (Figures 4J and 4K). Moreover, when we maintained the flies at 18°C during development and in adults, there were no reductions in ARI responses (18°→18°) (Figures 4J and 4K). These data demonstrate that the opsins are needed in the adult for the gustatory responses to ARI, and the mutants do not cause deficits in ARI taste because of a role for opsins during development.

To provide an additional test of the finding that the *opsin* mutations do not cause a developmental defect in GRNs, we examined responses to other bitter compounds that are detected by the same GRNs as ARI. We found that the S6 sensilla from the *opsin* triple mutant ($rh7^{1}$,$rh4^{1}$,$rh1^{l17}$) showed a similar number of action potentials to denatonium, strychnine, and quinine as control flies (Figures S4A–S4C). Given that there is only one bitter-responsive GRN in these sensilla, these results demonstrate that this GRN was still functional in the triple mutant and specifically lacked a response to ARI. Consistent with these results, the avoidances to denatonium, strychnine, and quinine were indistinguishable between control and $rh7^{1}$,$rh4^{1}$,$rh1^{l17}$ flies (Figures S4E–S4G). The triple mutant also exhibited normal gustatory responses to sucrose (Figures S4D and S4H). Further indicating that the deficit in ARI taste is not due to a developmental defect, the morphology of *Gr66a-positive* GRNs, including the bitter-responsive GRN in S6 sensilla, were indistinguishable between the *opsin* mutants and the control (Figures S4I–S4L).

Given that we used the *opsin-GAL4*s to rescue the various opsin phenotypes, yet the drivers were not sufficiently strong to reveal reporter staining, the question arises as to whether the *GAL4*s are capable of driving expression in the labellum. To address this issue, we focused on the *rh1-GAL4* and conducted RT-qPCR

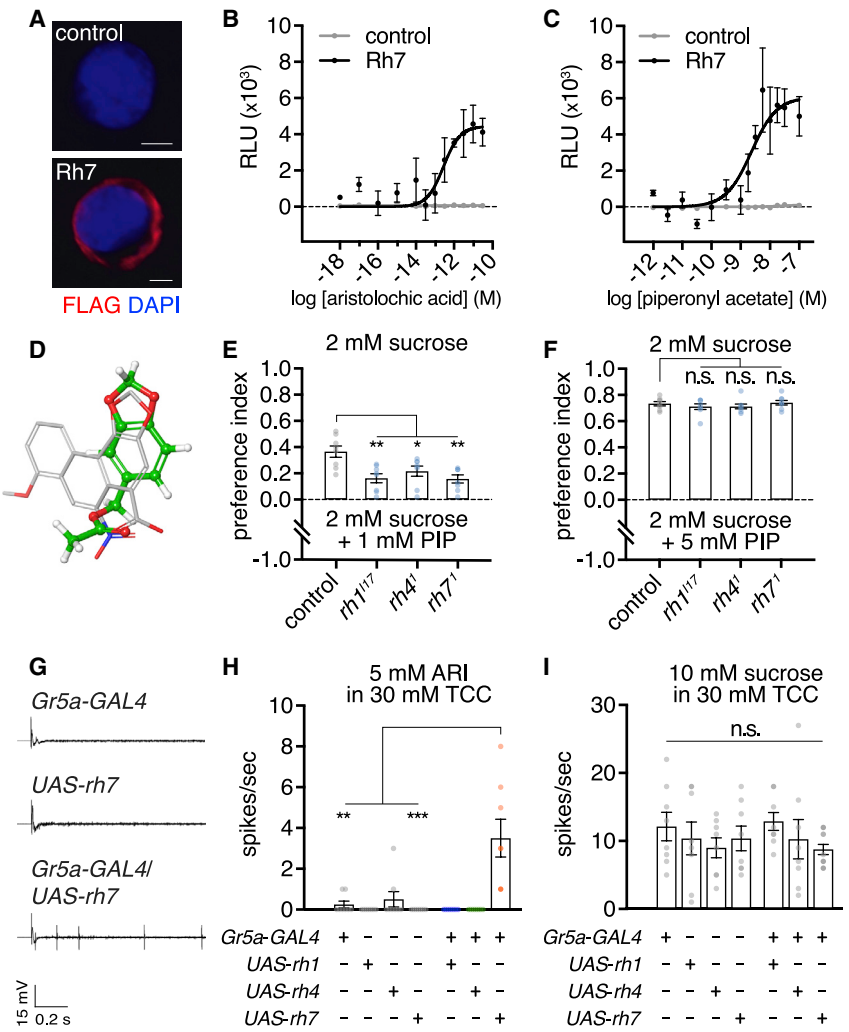

Figure 5. Activation of Rh7 *In Vitro*

(A) HEK293T cells expressing the empty vector (control; top) and the vector encoding FLAG::Rh7 (bottom). Anti-FLAG (red) and DAPI nuclear stain (blue). Scale bars indicate 5 μm. See also Figures S5A and S5B.

(B and C) Normalized dose responses of control cells (gray) and FLAG::Rh7-expressing cells (black) stimulated with (B) ARI and (C) PIP. Activities assessed using a β-arrestin recruitment assay [31]. Signals are normalized to the vehicle control baseline. n = 4 per concentration. Means ± SEMs. Abbreviations are as follows: RLU, relative luminescence units.

(D) Superimposition of the PIP (green) and ARI structures (white). See also Figures S5C and S5D.

(E and F) Testing preferences of control, $rh1^{I17}$, $rh4^{1}$, and $rh7^{1}$ flies for 2 mM sucrose versus 2 mM sucrose plus (E) 1 mM PIP or (F) 5 mM PIP by using two-way choice feeding assays. n = 8 per genotype. Means ± SEMs. Statistics were performed by using one-way ANOVA with Tukey's multiple comparisons tests.

(G) Representative tip recording traces obtained by stimulating L4 sensilla of the indicated flies with 5 mM ARI in 30 mM TCC.

(H) Quantification of tip recording action potentials of flies ectopically expressing *rh1*, *rh4*, or *rh7* in sugar-responsive neurons (using the *Gr5a-GAL4*) between 200–1,200 ms after application of 5 mM ARI in 30 mM TCC to L4 sensilla. n = 8 per genotype. Means ± SEM. Statistics were performed by using Kruskal-Wallis test with the Dunn's multiple comparisons test.

(I) Quantification of tip recording action potentials of flies ectopically expressing *rh1*, *rh4*, or *rh7* in sugar-responsive neurons (using the *Gr5a-GAL4*) between 200–1,200 ms after application of 100 mM sucrose in 30 mM TCC to L4 sensilla. n = 8 per genotype. Means ± SEMs. Statistics were performed by using one-way ANOVA with a Tukey's multiple comparisons test.

*p < 0.05, **p < 0.01, and ***p < 0.001.

experiments using the *rh1-GAL4* and *UAS-rh1* in a null $rh1^{I17}$ background. We observed increases in *rh1* transcript levels in the labella of *rh1-GAL4* > *UAS-rh1;*$rh1^{I17}$ flies compared with flies harboring the *UAS-rh1* transgene only in a $rh1^{I17}$ background (Figure S4M). These data indicate that the *rh1-GAL4* directs expression in the labellum, thereby providing an explanation as to how the driver can rescue the phenotype. The presence of low levels of *rh1* transcripts in control flies (*UAS-rh1;*$rh1^{I17}$) is presumably due to residual genomic DNA in the RNA preparation, after DNase I treatment.

Activation of Rh7 by Bitter Compounds *In Vitro*

To test whether the opsins are chemical receptors, we set out to express them in tissue culture cells to determine whether they are activated by ARI. Functional expression of most *Drosophila* opsins in heterologous systems has not been successful because of their inability to exit the endoplasmic reticulum. Indeed, Rh1 and Rh4 remain in the endoplasmic reticulum when expressed in HEK293T cells (Figures S5A and S5B). However, we can effectively express Rh7 and detect an extracellular N-terminal FLAG tag (Figure 5A) [22]. We did not detect either Rh1 or Rh4 on the cell surface even after substituting the N- and C-terminal regions of these opsins with the corresponding versions of Rh7 (Figures S5A and S5B). Moreover, Rh7 was also retained in the endoplasmic reticulum of HEK293T cells when co-expressed with Rh1 or Rh4. Therefore, we focused the following analysis on Rh7.

To determine whether Rh7 can be activated by ARI, we used an approach that takes advantage of β-arrestin binding to an activated GPCR [31]. In this assay, β-arrestin is fused to a TEV protease, whereas the GPCR is linked to a tTA transcriptional activator with an intervening tobacco etch virus protease cleavage site (TEVpcs). Upon recruitment of the β-arrestin-TEV protease fusion protein to the activated GPCR-TEVpcs-tTA chimera, the tTA is released from the GPCR, leading to expression of a luciferase reporter.

We found that Rh7 was activated by ARI in a dose-dependent manner (half maximal effective concentration (EC_{50}) = 0.28 pM) (Figure 5B). Piperonyl acetate (PIP) is structurally similar to ARI (Figure 5D) and is a bitter compound [32]. Rh7 was also activated by PIP (EC_{50} = 2.29 nM) (Figure 5C). Consistent with these data, 1 mM PIP is repulsive to control flies, and this aversion is significantly reduced in *opsin* mutant flies (Figures 5E).

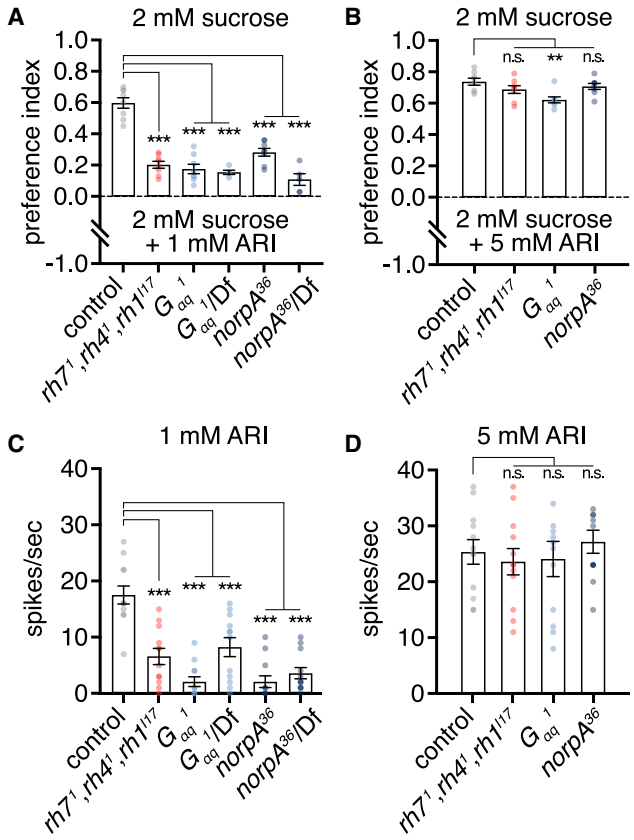

Figure 6. G_q-PLCβ signaling functions in sensation of lower concentrations of aristolochic acid

(A and B) Two-way choice feeding assays testing the preferences for 2 mM sucrose versus 2 mM sucrose plus (A) 1 mM ARI or (B) 5 mM ARI. n = 5–8 per genotype. Df indicates a deficiency line. Means ± SEMs. Statistics for the *opsin* triple mutant was performed using the unpaired Student's t test. The statistics for $G_{\alpha q}$ and *norpA* alleles were performed using one-way ANOVA with Tukey's multiple comparisons test.

(C and D) Quantification of tip recording action potentials between 200–1,200 ms after application of (C) 1 mM ARI or (D) 5 mM ARI. n = 12 per genotype. Means ± SEMs. The statistics for the *opsin* triple mutant was performed using the Mann-Whitney test. The statistics for the $G_{\alpha q}$ and *norpA* alleles were performed by using the Kruskal-Wallis test with Dunn's multiple comparisons test. See also Figure S6.

**p < 0.01 and ***p < 0.001.

We also tested whether ectopic expression of any of the opsins *in vivo* confers responsiveness to ARI. Sugar-responsive GRNs express PLC [33, 34]. Therefore, we expressed *UAS-rh1*, *UAS-rh4*, or *UAS-rh7* under control of the *Gr5a-GAL4* driver, which is expressed in sugar-responsive GRNs [35]. We found that expression of *rh7*, but not *rh1* or *rh4*, generated aristolochic-acid-induced action potentials (Figures 5G and 5H). Moreover, the response by sugar-responsive GRNs expressing *rh7* required a high concentration of ARI (5 mM), and the frequency of action potentials was relatively low (Figure 5H) (3.5 ± 0.9 spikes per second). The low frequency of action potentials was not due to impairments in the sugar GRNs given that the flies exhibited normal sucrose responses (Figure 5I). The results that only Rh7-expressing sugar GRNs display aristolochic-acid-induced action potentials is consistent with our findings that in HEK293 cells, Rh7 is functionally expressed but Rh1 and Rh4 are retained in the endoplasmic reticulum. Furthermore, the low sensitivity of Rh7-expressing sugar-responsive GRNs to ARI supports the mutant analyses in bitter GRNs, suggesting that all three opsins are required in the same cells for high sensitivity to this chemical.

Modeling of Bitter Compound Binding to Rh7

We performed homology modeling of Rh7 by using the crystal structures of human, bovine, and squid rhodopsins as templates (GPCR-I-TASSER) [36]. Using induced-fit docking simulations, we investigated the ARI and PIP binding to the GPCR orthosteric ligand pocket and found that both chemicals fit into a similar binding pocket as retinal (Figures S5C and S5D). ARI appeared to establish polar interactions with K374 and hydrophobic interactions with F286 and Y346 (Figure S5C). Most of the residues in Rh7 that are predicted to interact with ARI are conserved in Rh1 and Rh4 (Table S2). PIP appears to interact with the same residues, including a hydrogen bond with K374 and aromatic interactions with F286 and Y346 (Figure S5D).

Opsins Couple to a Signaling Cascade to Sense Lower Concentrations of Aristolochic Acid

In photoreceptor cells, rhodopsin-dependent signaling amplifies responses to dim light. Therefore, we wondered whether Rh1, Rh4, and Rh7 were specifically required for sensing lower amounts of ARI. We compared the behavior of the *opsin* triple mutant flies by using 1 mM and 5 mM ARI. In contrast to the strong impairment in response to 1 mM ARI, $rh7^1$,$rh4^1$,$rh1^{117}$ flies did not show a significant deficit in avoiding 5 mM ARI (Figures 6A and 6B) (PI = 0.20 ± 0.02 and 0.69 ± 0.02, respectively). These results were mirrored by concentration-dependent effects on neuronal firing of GRNs. Elimination of the opsins caused a dramatic attenuation in action potentials in response to 1 mM ARI (Figures 6C and S6A) (6.6 ± 1.4 spikes per second), whereas the triple mutant displayed normal neuronal activity upon exposure to 5 mM ARI (Figures 6D and S6B) (23.6 ± 2.3 spikes per second). The *opsin* mutants also responded normally to the higher concentration of PIP (5 mM) (Figure 5F).

The rhodopsins in fly photoreceptor cells initiate a signaling cascade that engages a trimeric G protein (G_q), a PLC-β (no receptor potential A [NORPA]), and culminates with activation of the TRP and TRPL channels [37–41]. Therefore, the opsins might couple to a similar pathway in GRNs. If so, $G_{\alpha q}$ and NORPA might function in GRNs for sensing lower (1 mM) but not higher (5 mM) concentrations of ARI. We assayed behavioral responses and neuronal firing in $G_{\alpha q}{}^1$ and $norpA^{36}$ mutant flies, along with each mutant over the corresponding deficiency and found large reductions in avoidance and action potentials to 1 mM ARI (Figures 6A, 6C, and S6A). However, these flies responded normally to 5 mM ARI, with the exception of $G_{\alpha q}{}^1$ mutant flies, which exhibited a slight defect in the behavioral response only (Figures 6B, 6D, and S6B).

Mutation of *trpA1-CD* Disrupts Aristolochic Acid Taste

We previously showed that the gustatory avoidance of ARI depends on TRPA1 [6]. Our data suggest that lower amounts of ARI (1 mM) primarily activate TRPA1 indirectly given that the responses to this concentration depend on opsins, $G_{\alpha q}$, and NORPA. However, TRPA1 might be effectively activated directly by 5 mM ARI given that the detection of this concentration is

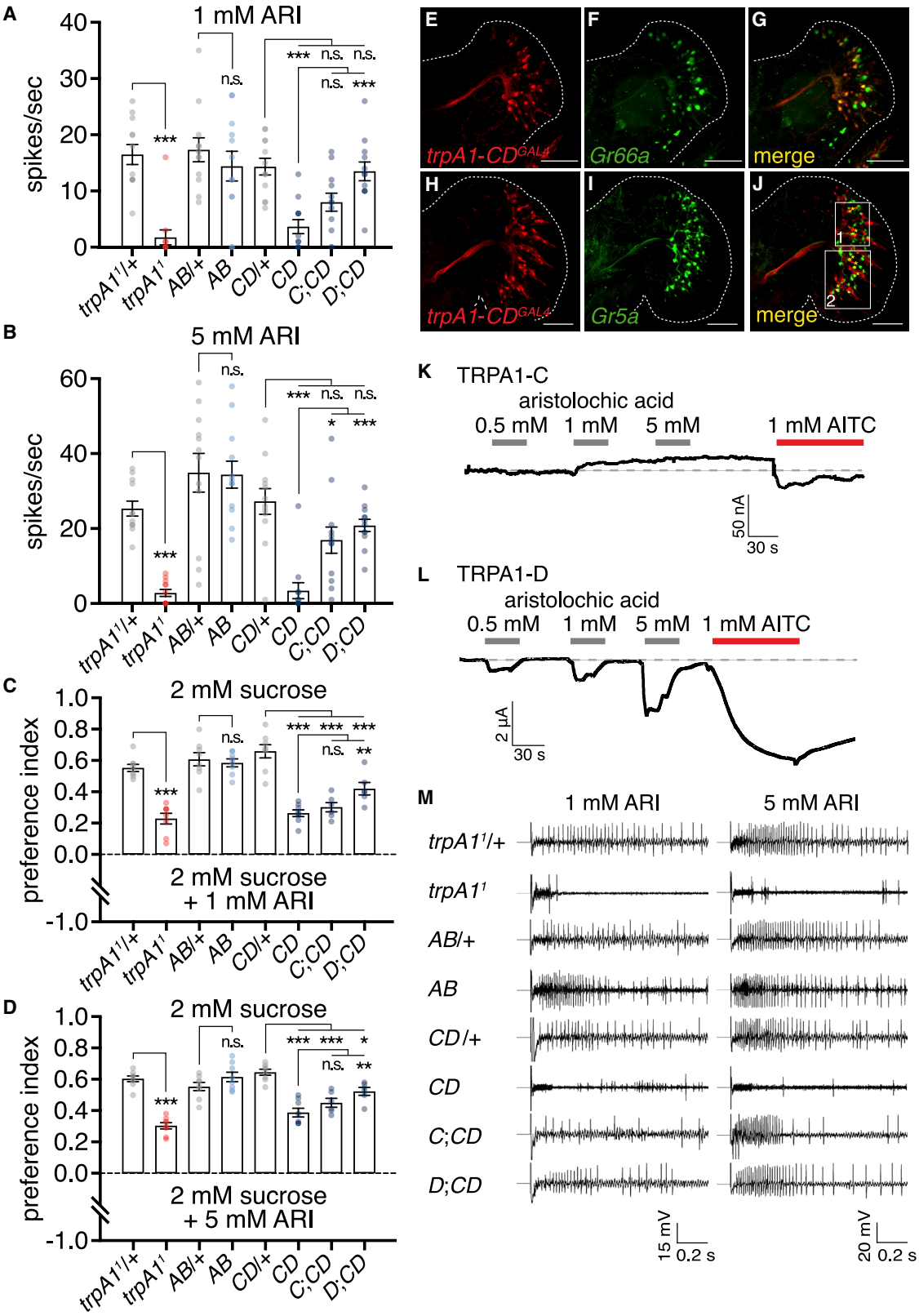

Figure 7. Role of TRPA1 Isoforms in Sensing Aristolochic Acid

Testing requirements for *trpA1* isoforms in responding to ARI: *trpA1*^{1} (null mutant), *trpA1-AB*^{GAL4} (*AB*; disrupting *A* and *B* isoforms; see also Figure S7C), *trpA1-CD*^{GAL4} (*CD*; disrupting *C* and *D* isoforms; see also Figure S7C), and the *trpA1-CD*^{GAL4} mutant expressing either the *UAS-trpA1-C* (*C*;*CD*) or *UAS-trpA1-D* (*D*;*CD*) transgenes.

(legend continued on next page)

independent of the opsins, $G_{\alpha q}$ and NORPA. Therefore, we tested whether the *trpA1*^{1} null mutant displays impairments in the responses to 1 mM and 5 mM ARI. We found that at both of these concentrations, aristolochic-acid-induced action potentials were nearly eliminated (Figures 7A, 7B and 7M). Although the electrophysiological responses to ARI are virtually eliminated in the *trpA1*^{1} mutant, there is a remaining aversion to ARI (Figures 7C and 7D). The behavioral avoidance in the *trpA1*^{1} mutant is most likely due to the observations that, in addition to activating bitter-responsive GRNs, which induces aversion, bitter compounds also suppress sugar-responsive GRNs, thereby decreasing attraction to sugars [42–44].

We combined each *opsin* mutation with *trpA1*^{1} and found that in response to 1 mM ARI, the double mutants showed comparable electrophysiological phenotypes to *trpA1*^{1} alone, consistent with the conclusion that they function in a common pathway (Figure S7A). Because the opsins are dispensable for responding to 5 mM ARI, the double mutants also showed similar deficits in the electrophysiological responses as the *trpA1*^{1} mutant alone (Figure S7B). Further evidence consistent with the model that the opsins and TRPA1 function in a common pathway, the chemical specificity of TRPA1 was reminiscent of the opsins, given that TRPA1 was not required for the responses to denatonium, strychnine, denatonium (Figures S4A–C and S4E–G), or sucrose (Figures S4D and S4H).

The *trpA1* gene encodes several isoforms [45]. The A and B isoforms (AB) share a common promoter [45–48], while the C and D isoforms (CD) share a different promoter [45, 47, 48] (Figure S7C). We found that removal of the AB isoforms (*trpA1-AB*^{GAL4}) had no effect on the avoidance or electrophysiological responses to 1 mM or 5 mM ARI (Figures 7A–7D and 7M). In contrast, deletion of the CD isoforms (*trpA1-CD*^{GAL4}) significantly impaired repulsion and reduced neuronal firing to 1 mM and 5 mM ARI, similar to the *trpA1*^{1} mutant (Figures 7A–7D and 7M).

Expression Patterns of *trpA1* Isoforms

To address whether the *trpA1-CD* isoforms are expressed in GRNs in the labellum, we used the *GAL4* knock-in (*trpA1-CD*^{GAL4}) to drive expression of *UAS-dsRed*. We found that the *CD*^{GAL4} reporter was broadly expressed in GRNs (Figure 7E). A subset of these GRNs overlapped with a marker that labels bitter-responsive GRNs (*Gr66a-I-GFP*) (Figures 7F and 7G), but not with a marker that labeled sugar-responsive GRNs (*Gr5a-I-GFP*) (Figures 7H–7J and S7J). The *GAL4* reporter for the *trpA1-AB* isoforms (*trpA1-AB*^{GAL4}) drove expression of *UAS-dsRed* in a subset of bitter-responsive GRNs, but not the sugar-responsive GRNs (Figures S7D–S7I and S7K).

We examined the distribution of the *AB*^{GAL4} and *CD*^{GAL4} reporters in the brain and legs by using the *UAS-mCD8::GFP* reporter. In the brain, the *AB*^{GAL4} labeled the fan-shaped body (FB) and the gustatory center—the subesophageal zone (SEZ) (Figure S7M)—and the *CD*^{GAL4} stained the SEZ and antennal lobes (AL) (Figure S7O). We also examined expression of the *AB*^{GAL4} and *CD*^{GAL4} reporters in the tarsal segments of the pro-thoracic legs. The cuticle of the tarsi produces autofluorescence with *UAS-GFP* only, but there is no autofluorescence corresponding to cells (Figure S7L). The *AB*^{GAL4} fluorescent was indistinguishable from the *UAS-GFP*-only control (Figures S7N and S7N'), whereas the *CD*^{GAL4} stained neuronal processes and cell bodies in multiple segments (Figure S7P).

Activation of TRPA1-D by Aristolochic Acid

The preceding data suggest that either the TRPA1-C or TRPA1-D isoform might be directly activated by ARI, and more robustly at the higher (5 mM) than lower amounts (1 mM). We expressed these proteins in *Xenopus* oocytes and performed two-electrode voltage clamp recordings. Unlike many TRPA1 isoforms that are strongly activated by allyl isothiocyanate (AITC) [49–51], TRPA1-C is very mildly responsive to AITC and showed no activity upon addition of ARI, even at a concentration of 5 mM (Figure 7K). However, TRPA1-D, which was robustly stimulated by AITC, showed dose-dependent activation by ARI starting at 0.5 mM and was strongly responsive at 5 mM (Figure 7L). Moreover, we restored normal behavioral and electrophysiological responses to 1 mM and 5 mM ARI in *trpA1-CD*^{GAL4} mutant flies by expressing the *UAS-trpA1-D* transgene under control of the *GAL4* knocked into the *trpA1-CD*^{GAL4} allele (Figures 7A–7D; labeled *D*;*CD*). Unexpectedly, we observed partial rescue by using the *trpA1-C* transgene (Figures 7A–7D; labeled *C*;*CD*). Therefore, although we cannot exclude a role for the C isoform, we conclude that TRPA1-D is directly activated by ARI.

DISCUSSION

Opsin Apoprotein Functions Independent of Retinal in Taste

In this study, we demonstrate that opsins function in *Drosophila* taste. In support of this conclusion, mutation of *rh1*, *rh4*, or *rh7*

(A and B) Quantification of tip recording action potentials between 200–1,200 ms following application of (A) 1 mM ARI and (B) 5 mM ARI. n = 12 per genotype. Means ± SEMs. Statistics for *trpA1* and *AB* were performed using the Mann-Whitney test. Statistics for *CD* and *CD* isoform rescues were performed using the Kruskal-Wallis test with Dunn's multiple comparisons test.

(C and D) Two-way choice feeding assays testing the preferences for 2 mM sucrose alone versus 2 mM sucrose plus (C) 1 mM ARI and (D) 5 mM ARI. n = 6–8 per genotype. Means ± SEMs. Statistics for *trpA1* and *AB* were performed using the unpaired Student's t test. Statistics for the *CD* and *CD* isoform rescues were performed using one-way ANOVA with Tukey's multiple comparisons test.

(E–G) Confocal images of labella showing expression of (E) *UAS-dsRed* driven by *trpA1-CD*^{GAL4}, (F) *Gr66a-I-GFP*, and (G) merge. Tissues were stained with anti-dsRed (red) and anti-GFP (green). Scale bars indicate 50 μm.

(H–J) Confocal images of labella showing expression of (H) *UAS-dsRed* driven by *trpA1-CD*^{GAL4}, (I) *Gr5a-I-GFP*, and (J) merge. Tissues were stained with anti-dsRed (red) and anti-GFP (green). Scale bars indicate 50 μm. Asterisks indicate separate cell bodies that do not co-label. See Figure S7J for boxed regions.

(K and L) Two-electrode voltage clamp recordings using *Xenopus* oocytes injected with (K) *trpA1-C* or (L) *trpA1-D* cRNA. The oocytes were perfused with the indicated concentrations of ARI followed by 1 mM allyl isothiocyanate (AITC). Shown are the whole-cell inward currents.

(M) Representative tip recording traces of Figures 7A and 7B obtained by stimulating S6 sensilla with 1 mM ARI and 5 mM ARI, respectively. The genotypes are indicated.

*p < 0.05, **p < 0.01, and ***p < 0.001.

reduced the behavioral and electrophysiological responses to lower amounts of ARI. The opsins function in GRNs given that we fully rescued the mutant phenotypes by introducing wild-type transgenes specifically in bitter-responsive GRNs. Although we detected opsin transcripts in the labellum, opsin expression was below the levels detectable with antibodies or with the *opsin* reporters. We propose that the low expression of opsins in GRNs provides a mechanism to prevent light from interfering with gustatory responses. Consistent with this proposal, the functions of opsins in GRNs are light independent.

In photoreceptor cells, opsins bind to retinal, which is the light-sensitive component of rhodopsin. In fly eyes, retinal is also required for rhodopsins to exit the endoplasmic reticulum [24]. In thermosensory, auditory, and proprioceptive neurons that depend on rhodopsins for temperature discrimination, hearing, and locomotion, the retinal is also essential, even though the roles of rhodopsins in these neurons are light independent [11–14]. Presumably, this reflects the chaperone function of the retinal. However, the chromophore is not required for the function of opsins in chordotonal neurons [52].

We found that retinal is dispensable in GRNs for opsin function given that *ninaD*^{1} mutants raised on carotenoid-free food respond normally to ARI. Moreover, mutation of the lysine critical for binding retinal does not prevent detection of ARI by Rh1. Therefore, retinal does not serve as a molecular chaperone for opsins in GRNs. An open question concerns the molecular and cellular explanation as to how opsins can bypass a chaperone requirement for retinal in some neurons, such as GRNs and chordotonal neurons.

Opsins Are Chemosensors

An important issue is whether or not opsins function directly as chemosensors. This is challenging to address given that *in vitro* expression of most insect opsins is problematic because they are not trafficked to the plasma membrane. Rh7 is an exception because it can be functionally expressed in HEK293T cells [22]. We demonstrate that ARI and a structurally similar chemical, PIP, stimulate dose-dependent increases in Rh7 activity. On the basis of these findings, we propose that Rh7 is activated directly by ARI and PIP. Our structural modeling suggests that these ligands occupy a similar binding site as retinal. The observation that retinal is dispensable for sensing these tastants supports this model, given that the retinal binding site is available for binding other ligands. Rh7 might be part of a heteromultimeric receptor that includes Rh1 and Rh4, and the sensitivity for ARI and PIP might be increased by a heteromultimeric opsin receptor. However, it was not possible to functionally express Rh1 or Rh4 in HEK293T cells because they are retained in the endoplasmic reticulum.

Functioning of Multiple Opsins in the Same Bitter-Responsive GRNs

In support of the conclusion that Rh1, Rh4, and Rh7 function in the same GRNs, we found that we could rescue the phenotype of each mutant by driving expression of the corresponding wild-type transgene with the transcriptional control region of a different *opsin* gene. Co-function of multiple opsins in the same GRNs differs from most photoreceptor cells [21]. However, Rh3 and Rh4 act together in a subset of photoreceptor cells near the dorsal rim of the *Drosophila* eye [53], and rhodopsins are co-expressed in R7 cells of mosquitoes [54] Moreover, two or more opsins function in the same thermosensory, auditory, and proprioceptive neurons in flies [11–14]. Two visual pigments (S and M opsins) are also co-expressed in a subset of mouse cone cells [55].

Until recently, GPCRs were generally thought to be comprised of homo- or heterodimers [reviewed in 56–58]. However, a series of recent studies indicate that at least some GPCRs function as tetramers through association of two homo- and/or heterodimers [59–65]. Thus, three opsins might form a heteromultimer in GRNs. The concept that bitter taste receptors consist of more than two subunits might also extend to the mammalian bitter receptors, T2Rs, which are GPCRs. Multiple T2Rs respond to the same bitter compound and appear to be co-expressed in the same taste receptor cells [66–69].

Evolutionary Conservation of GPCR Signaling in Taste

Many mammals, such as mice and humans, sense bitter, sweet, and umami tastes through signaling cascades that include GPCRs, G_q, PLC, and TRP channels [reviewed in 1]. This differs from gustatory sensation in flies, which is accomplished primarily through activation of ionotropic receptors, such as ''gustatory receptors'' (GRs). Our findings that Rh1, Rh4, and Rh7 operate in sensing ARI through a cascade that also includes a G_q, PLC, and a TRP channel demonstrate that the repertoire of gustatory strategies used by flies includes a signaling cascade reminiscent of mammalian taste transduction. Thus, GPCR signaling in taste is evolutionarily conserved from flies to humans and represents an ancient strategy to evaluate the chemical composition of food.

Logic for Dual TRPA1 Mechanisms for Sensing Different Amounts of the Same Tastant

A key question concerns the logic for flies to employ both opsins and an ionotropic receptor (TRPA1) for sensing gustatory stimuli. Gustatory detection of both the lower (1 mM) and higher (5 mM) amounts of ARI depends on TRPA1. 1 mM ARI, which is not very effective at directly activating TRPA1-D *in vitro*, is primarily sensed in GRNs through opsins. The *trpA1* single mutant or *opsin* and *trpA1* double mutants showed the same reduction in action potentials in response to 1 mM ARI, indicating that the opsins function in a common pathway with TRPA1. Nevertheless, in the absence of opsins, 1 mM ARI induces a low frequency of action potentials in GRNs. This small response presumably occurs because 1 mM ARI is sufficient to elicit a minor level of direct activation of TRPA1-D.

When flies are presented with 5 mM ARI, the opsins, Gq, and PLC are dispensable. This is consistent with our finding that this higher amount of ARI is sufficient to robustly activate TRPA1-D directly. At higher amounts of ARI, the opsins might undergo Ca^{2+}-mediated feedback regulation, thereby attenuating their activities. Because TRPA1 is directly activated by ARI, the existence of this ionotropic mechanism for responding to ARI could provide a backup mechanism, allowing for responses to ARI at high concentrations that largely eliminate opsin activities through adaptation.

We propose that the opsin-initiated signaling cascade in GRNs provides signal amplification. In fly photoreceptor cells, light activation of a single rhodopsin leads to successive

engagement of ~5 $G_{\alpha q}$ subunits, each of which stimulates one PLC [70]. The cascade culminates in activating many TRP and TRPL channels. Similarly, in fly GRNs, opsins couple to G_q, PLC, and a TRP channel (TRPA1), but only in response to lower amounts of ARI. Our finding that low amounts activate Rh7 in HEK293T cells supports the proposal that an opsin-initiated signaling cascade in GRNs facilitates signal amplification. This provides greater sensitivity than would be possible if direct activation of TRPA1 were the only mechanism for sensing ARI.

Archetypal Role for Opsins

We propose that the primordial opsins were chemosensors rather than light sensors. Chemical sensation is ancient, and most likely preceded light sensation. We suggest that the primordial opsins bound chemicals and these proteins were subsequently co-opted as light sensors because of interaction with a chemical ligand (retinal), which underwent a light-induced conformational change, thereby conferring light sensitivity to the opsin. Indeed, there are primitive but extant organisms, such as comb jellies, that express many opsins in cells that do not appear to function in light sensation [71–73].

Potential Roles for Opsins in Mammalian Taste

Multiple mammalian opsins are expressed outside of the retina [73]. These include Opn3 and Opn5, which are expressed in the brain and spinal cord [74–76]. Mammalian opsins are also expressed in immune cells, liver, lungs, testis, and the aorta, although their roles are mysterious [74–79]. Moreover, although not mentioned in the text of the publications, transcriptome analyses of mammalian taste bud cells and taste organoids reveal *opsin* RNAs in these gustatory tissues [80, 81]. These results, in combination with our findings in flies, raise the exciting prospect that opsins represent a new class of taste receptor in mammalian taste buds.

STAR★METHODS

Detailed methods are provided in the online version of this paper and include the following:

- KEY RESOURCES TABLE
- LEAD CONTACT AND MATERIALS AVAILABILITY
- EXPERIMENTAL MODEL AND SUBJECT DETAILS
  - Fly stocks
  - Fly husbandry
  - Cell lines
- METHOD DETAILS
  - Generating *UAS-rh1*^{K319R}
  - Two-way choice feeding assays
  - Extracellular tip recordings
  - Chemicals for feeding assays and tip recordings
  - Cell culture and β-arrestin recruitment assay
  - Aristolochic acid analogs
  - Homology modeling of Rh7
  - Quantitative PCR
  - Immunostaining
  - Recipe for carotenoid-deficient food
  - Electroretinogram recordings
  - Two-electrode voltage clamp recordings
- QUANTIFICATION AND STATISTICAL ANALYSIS
- DATA AND CODE AVAILABILITY

SUPPLEMENTAL INFORMATION

Supplemental Information can be found online at https://doi.org/10.1016/j.cub.2020.01.068.

ACKNOWLEDGMENTS

We thank Wesley Kroeze and Bryan Roth for providing HTLA cells and guidance for the TANGO assay, and Chao Liu for conducting preliminary studies. N.Y.L. was partially supported by a predoctoral fellowship from the National Eye Institute (F31EY027191). M.Y.N. received an Israel Science Foundation grant (494/16). This work was supported by grants to CM from the National Institute on Deafness and Other Communication Disorders (DC007864 and DC016278).

AUTHOR CONTRIBUTIONS

Conceptualization, N.Y.L., S.H.K., and C.M.; Methodology, N.Y.L., A.D.P., M.Y.N., and C.M.; Validation, N.Y.L.; Formal Analysis, N.Y.L.; Investigation, N.Y.L., D.T., A.S.G., A.D.P., and M.Y.N.; Writing – Original Draft, N.Y.L. and C.M.; Writing – Review & Editing, N.Y.L., A.D.P., M.Y.N., and C.M.; Visualization, N.Y.L. and C.M.; Supervision, C.M.; Project Administration, C.M.; Funding acquisition, C.M.

DECLARATION OF INTERESTS

The authors declare no competing interests.

Received: November 18, 2019
Revised: January 16, 2020
Accepted: January 22, 2020
Published: April 2, 2020

REFERENCES

1. Liman, E.R., Zhang, Y.V., and Montell, C. (2014). Peripheral coding of taste. Neuron *81*, 984–1000.
2. Zhang, Y., Hoon, M.A., Chandrashekar, J., Mueller, K.L., Cook, B., Wu, D., Zuker, C.S., and Ryba, N.J. (2003). Coding of sweet, bitter, and umami tastes: different receptor cells sharing similar signaling pathways. Cell *112*, 293–301.
3. Pérez, C.A., Huang, L., Rong, M., Kozak, J.A., Preuss, A.K., Zhang, H., Max, M., and Margolskee, R.F. (2002). A transient receptor potential channel expressed in taste receptor cells. Nat. Neurosci. *5*, 1169–1176.
4. Damak, S., Rong, M., Yasumatsu, K., Kokrashvili, Z., Pérez, C.A., Shigemura, N., Yoshida, R., Mosinger, B., Jr., Glendinning, J.I., Ninomiya, Y., and Margolskee, R.F. (2006). Trpm5 null mice respond to bitter, sweet, and umami compounds. Chem. Senses *31*, 253–264.
5. Dutta Banik, D., Martin, L.E., Freichel, M., Torregrossa, A.M., and Medler, K.F. (2018). TRPM4 and TRPM5 are both required for normal signaling in taste receptor cells. Proc. Natl. Acad. Sci. USA *115*, E772–E781.
6. Kim, S.H., Lee, Y., Akitake, B., Woodward, O.M., Guggino, W.B., and Montell, C. (2010). *Drosophila* TRPA1 channel mediates chemical avoidance in gustatory receptor neurons. Proc. Natl. Acad. Sci. USA *107*, 8440–8445.
7. Kühne, W. (1878). On the stable colours of the retina. J. Physiol. *1*, 109–212.
8. Boll, F. (1877). Zur anatomie und physiologie der retina. Anat. Physiol. *1877*, 4–36.
9. Boll, F. (1977). On the anatomy and physiology of the retina. Vision Res. *17*, 1249–1265.
10. Costanzi, S., Siegel, J., Tikhonova, I.G., and Jacobson, K.A. (2009). Rhodopsin and the others: a historical perspective on structural studies of G protein-coupled receptors. Curr. Pharm. Des. *15*, 3994–4002.

11. Zanini, D., Giraldo, D., Warren, B., Katana, R., Andrés, M., Reddy, S., Pauls, S., Schwedhelm-Domeyer, N., Geurten, B.R.H., and Göpfert, M.C. (2018). Proprioceptive opsin functions in *Drosophila* larval locomotion. Neuron *98*, 67–74.e4.
12. Senthilan, P.R., Piepenbrock, D., Ovezmyradov, G., Nadrowski, B., Bechstedt, S., Pauls, S., Winkler, M., Möbius, W., Howard, J., and Göpfert, M.C. (2012). *Drosophila* auditory organ genes and genetic hearing defects. Cell *150*, 1042–1054.
13. Sokabe, T., Chen, H.C., Luo, J., and Montell, C. (2016). A switch in thermal preference in *Drosophila* larvae depends on multiple rhodopsins. Cell Rep. *17*, 336–344.
14. Shen, W.L., Kwon, Y., Adegbola, A.A., Luo, J., Chess, A., and Montell, C. (2011). Function of rhodopsin in temperature discrimination in *Drosophila*. Science *331*, 1333–1336.
15. Lee, Y., Kim, S.H., and Montell, C. (2010). Avoiding DEET through insect gustatory receptors. Neuron *67*, 555–561.
16. Moon, S.J., Köttgen, M., Jiao, Y., Xu, H., and Montell, C. (2006). A taste receptor required for the caffeine response in vivo. Curr. Biol. *16*, 1812–1817.
17. Moon, S.J., Lee, Y., Jiao, Y., and Montell, C. (2009). A *Drosophila* gustatory receptor essential for aversive taste and inhibiting male-to-male courtship. Curr. Biol. *19*, 1623–1627.
18. Sung, H.Y., Jeong, Y.T., Lim, J.Y., Kim, H., Oh, S.M., Hwang, S.W., Kwon, J.Y., and Moon, S.J. (2017). Heterogeneity in the *Drosophila* gustatory receptor complexes that detect aversive compounds. Nat. Commun. *8*, 1484.
19. Weiss, L.A., Dahanukar, A., Kwon, J.Y., Banerjee, D., and Carlson, J.R. (2011). The molecular and cellular basis of bitter taste in *Drosophila*. Neuron *69*, 258–272.
20. Dunipace, L., Meister, S., McNealy, C., and Amrein, H. (2001). Spatially restricted expression of candidate taste receptors in the *Drosophila* gustatory system. Curr. Biol. *11*, 822–835.
21. Montell, C. (2012). *Drosophila* visual transduction. Trends Neurosci. *35*, 356–363.
22. Ni, J.D., Baik, L.S., Holmes, T.C., and Montell, C. (2017). A rhodopsin in the brain functions in circadian photoentrainment in *Drosophila*. Nature *545*, 340–344.
23. Harris, W.A., Ready, D.F., Lipson, E.D., Hudspeth, A.J., and Stark, W.S. (1977). Vitamin A deprivation and *Drosophila* photopigments. Nature *266*, 648–650.
24. Ozaki, K., Nagatani, H., Ozaki, M., and Tokunaga, F. (1993). Maturation of major *Drosophila* rhodopsin, ninaE, requires chromophore 3-hydroxyretinal. Neuron *10*, 1113–1119.
25. Kiefer, C., Sumser, E., Wernet, M.F., and Von Lintig, J. (2002). A class B scavenger receptor mediates the cellular uptake of carotenoids in *Drosophila*. Proc. Natl. Acad. Sci. USA *99*, 10581–10586.
26. Wang, T., Jiao, Y., and Montell, C. (2007). Dissection of the pathway required for generation of vitamin A and for *Drosophila* phototransduction. J. Cell Biol. *177*, 305–316.
27. Johnson, E.C., and Pak, W.L. (1986). Electrophysiological study of *Drosophila* rhodopsin mutants. J. Gen. Physiol. *88*, 651–673.
28. Wang, J.K., McDowell, J.H., and Hargrave, P.A. (1980). Site of attachment of 11-*cis*-retinal in bovine rhodopsin. Biochemistry *19*, 5111–5117.
29. Zuker, C.S., Cowman, A.F., and Rubin, G.M. (1985). Isolation and structure of a rhodopsin gene from D. melanogaster. Cell *40*, 851–858.
30. O'Tousa, J.E., Baehr, W., Martin, R.L., Hirsh, J., Pak, W.L., and Applebury, M.L. (1985). The *Drosophila ninaE* gene encodes an opsin. Cell *40*, 839–850.
31. Kroeze, W.K., Sassano, M.F., Huang, X.P., Lansu, K., McCorvy, J.D., Giguère, P.M., Sciaky, N., and Roth, B.L. (2015). PRESTO-Tango as an open-source resource for interrogation of the druggable human GPCRome. Nat. Struct. Mol. Biol. *22*, 362–369.
32. Burdock, G.A. (2009). Fenaroli's Handbook of Flavor Ingredients, Sixth Edition (Milton Park: Taylor & Francis).
33. Kain, P., Badsha, F., Hussain, S.M., Nair, A., Hasan, G., and Rodrigues, V. (2010). Mutants in phospholipid signaling attenuate the behavioral response of adult *Drosophila* to trehalose. Chem. Senses *35*, 663–673.
34. Masek, P., and Keene, A.C. (2013). *Drosophila* fatty acid taste signals through the PLC pathway in sugar-sensing neurons. PLoS Genet. *9*, e1003710.
35. Thorne, N., Chromey, C., Bray, S., and Amrein, H. (2004). Taste perception and coding in *Drosophila*. Curr. Biol. *14*, 1065–1079.
36. Zhang, J., Yang, J., Jang, R., and Zhang, Y. (2015). GPCR-I-TASSER: a hybrid approach to G protein-coupled receptor structure modeling and the application to the human genome. Structure *23*, 1538–1549.
37. Bloomquist, B.T., Shortridge, R.D., Schneuwly, S., Perdew, M., Montell, C., Steller, H., Rubin, G., and Pak, W.L. (1988). Isolation of a putative phospholipase C gene of *Drosophila*, *norpA*, and its role in phototransduction. Cell *54*, 723–733.
38. Hardie, R.C., and Minke, B. (1992). The *trp* gene is essential for a light-activated Ca^{2+} channel in *Drosophila* photoreceptors. Neuron *8*, 643–651.
39. Montell, C., and Rubin, G.M. (1989). Molecular characterization of the *Drosophila trp* locus: a putative integral membrane protein required for phototransduction. Neuron *2*, 1313–1323.
40. Niemeyer, B.A., Suzuki, E., Scott, K., Jalink, K., and Zuker, C.S. (1996). The *Drosophila* light-activated conductance is composed of the two channels TRP and TRPL. Cell *85*, 651–659.
41. Scott, K., Becker, A., Sun, Y., Hardy, R., and Zuker, C. (1995). $G_{q\,\alpha}$ protein function in vivo: genetic dissection of its role in photoreceptor cell physiology. Neuron *15*, 919–927.
42. Meunier, N., Marion-Poll, F., Rospars, J.P., and Tanimura, T. (2003). Peripheral coding of bitter taste in *Drosophila*. J. Neurobiol. *56*, 139–152.
43. Jeong, Y.T., Shim, J., Oh, S.R., Yoon, H.I., Kim, C.H., Moon, S.J., and Montell, C. (2013). An odorant-binding protein required for suppression of sweet taste by bitter chemicals. Neuron *79*, 725–737.
44. Chu, B., Chui, V., Mann, K., and Gordon, M.D. (2014). Presynaptic gain control drives sweet and bitter taste integration in *Drosophila*. Curr. Biol. *24*, 1978–1984.
45. Zhong, L., Bellemer, A., Yan, H., Ken, H., Jessica, R., Hwang, R.Y., Pitt, G.S., and Tracey, W.D. (2012). Thermosensory and nonthermosensory isoforms of *Drosophila melanogaster* TRPA1 reveal heat-sensor domains of a thermoTRP Channel. Cell Rep. *1*, 43–55.
46. Kwon, Y., Shim, H.S., Wang, X., and Montell, C. (2008). Control of thermotactic behavior via coupling of a TRP channel to a phospholipase C signaling cascade. Nat. Neurosci. *11*, 871–873.
47. Luo, J., Shen, W.L., and Montell, C. (2017). TRPA1 mediates sensation of the rate of temperature change in *Drosophila* larvae. Nat. Neurosci. *20*, 34–41.
48. Kang, K., Panzano, V.C., Chang, E.C., Ni, L., Dainis, A.M., Jenkins, A.M., Regna, K., Muskavitch, M.A., and Garrity, P.A. (2011). Modulation of TRPA1 thermal sensitivity enables sensory discrimination in *Drosophila*. Nature *481*, 76–80.
49. Bandell, M., Story, G.M., Hwang, S.W., Viswanath, V., Eid, S.R., Petrus, M.J., Earley, T.J., and Patapoutian, A. (2004). Noxious cold ion channel TRPA1 is activated by pungent compounds and bradykinin. Neuron *41*, 849–857.
50. Jordt, S.E., Bautista, D.M., Chuang, H.H., McKemy, D.D., Zygmunt, P.M., Högestätt, E.D., Meng, I.D., and Julius, D. (2004). Mustard oils and cannabinoids excite sensory nerve fibres through the TRP channel ANKTM1. Nature *427*, 260–265.
51. Kang, K., Pulver, S.R., Panzano, V.C., Chang, E.C., Griffith, L.C., Theobald, D.L., and Garrity, P.A. (2010). Analysis of *Drosophila* TRPA1 reveals an ancient origin for human chemical nociception. Nature *464*, 597–600.
52. Katana, R., Guan, C., Zanini, D., Larsen, M.E., Giraldo, D., Geurten, B.R.H., Schmidt, C.F., Britt, S.G., and Göpfert, M.C. (2019). Chromophore-independent roles of opsin apoproteins in *Drosophila* mechanoreceptors. Curr. Biol. *29*, 2961–2969.e4.
53. Mazzoni, E.O., Celik, A., Wernet, M.F., Vasiliauskas, D., Johnston, R.J., Cook, T.A., Pichaud, F., and Desplan, C. (2008). *Iroquois complex* genes induce co-expression of *rhodopsins* in *Drosophila*. PLoS Biol. *6*, e97.

54. Hu, X., Leming, M.T., Whaley, M.A., and O'Tousa, J.E. (2014). Rhodopsin coexpression in UV photoreceptors of *Aedes aegypti* and *Anopheles gambiae* mosquitoes. J. Exp. Biol. *217*, 1003–1008.
55. Applebury, M.L., Antoch, M.P., Baxter, L.C., Chun, L.L., Falk, J.D., Farhangfar, F., Kage, K., Krzystolik, M.G., Lyass, L.A., and Robbins, J.T. (2000). The murine cone photoreceptor: a single cone type expresses both S and M opsins with retinal spatial patterning. Neuron *27*, 513–523.
56. Fotiadis, D., Jastrzebska, B., Philippsen, A., Müller, D.J., Palczewski, K., and Engel, A. (2006). Structure of the rhodopsin dimer: a working model for G-protein-coupled receptors. Curr. Opin. Struct. Biol. *16*, 252–259.
57. Rivero-Müller, A., Jonas, K.C., Hanyaloglu, A.C., and Huhtaniemi, I. (2013). Di/oligomerization of GPCRs-mechanisms and functional significance. Prog. Mol. Biol. Transl. Sci. *117*, 163–185.
58. Franco, R., Martínez-Pinilla, E., Lanciego, J.L., and Navarro, G. (2016). Basic pharmacological and structural Evidence for class A G-protein-coupled receptor heteromerization. Front. Pharmacol. *7*, 76.
59. Damian, M., Pons, V., Renault, P., M'Kadmi, C., Delort, B., Hartmann, L., Kaya, A.I., Louet, M., Gagne, D., Ben Haj Salah, K., et al. (2018). GHSR-D2R heteromerization modulates dopamine signaling through an effect on G protein conformation. Proc. Natl. Acad. Sci. USA *115*, 4501–4506.
60. Lambert, N.A. (2010). GPCR dimers fall apart. Sci. Signal. *3*, pe12.
61. Redka, D.S., Morizumi, T., Elmslie, G., Paranthaman, P., Shivnaraine, R.V., Ellis, J., Ernst, O.P., and Wells, J.W. (2014). Coupling of g proteins to reconstituted monomers and tetramers of the M_2 muscarinic receptor. J. Biol. Chem. *289*, 24347–24365.
62. Pétrin, D., and Hébert, T.E. (2012). The functional size of GPCRs - monomers, dimers or tetramers? Subcell. Biochem. *63*, 67–81.
63. Navarro, G., Cordomí, A., Zelman-Femiak, M., Brugarolas, M., Moreno, E., Aguinaga, D., Perez-Benito, L., Cortés, A., Casadó, V., Mallol, J., et al. (2016). Quaternary structure of a G-protein-coupled receptor heterotetramer in complex with G_i and G_s. BMC Biol. *14*, 26.
64. Cordomí, A., Navarro, G., Aymerich, M.S., and Franco, R. (2015). Structures for G-protein-coupled receptor tetramers in complex with G proteins. Trends Biochem. Sci. *40*, 548–551.
65. Sleno, R., and Hébert, T.E. (2019). Shaky ground - The nature of metastable GPCR signalling complexes. Neuropharmacology *152*, 4–14.
66. Yarmolinsky, D.A., Zuker, C.S., and Ryba, N.J. (2009). Common sense about taste: from mammals to insects. Cell *139*, 234–244.
67. Adler, E., Hoon, M.A., Mueller, K.L., Chandrashekar, J., Ryba, N.J., and Zuker, C.S. (2000). A novel family of mammalian taste receptors. Cell *100*, 693–702.
68. Mueller, K.L., Hoon, M.A., Erlenbach, I., Chandrashekar, J., Zuker, C.S., and Ryba, N.J. (2005). The receptors and coding logic for bitter taste. Nature *434*, 225–229.
69. Meyerhof, W., Batram, C., Kuhn, C., Brockhoff, A., Chudoba, E., Bufe, B., Appendino, G., and Behrens, M. (2010). The molecular receptive ranges of human TAS2R bitter taste receptors. Chem. Senses *35*, 157–170.
70. Yau, K.W., and Hardie, R.C. (2009). Phototransduction motifs and variations. Cell *139*, 246–264.
71. Feuda, R., Rota-Stabelli, O., Oakley, T.H., and Pisani, D. (2014). The comb jelly opsins and the origins of animal phototransduction. Genome Biol. Evol. *6*, 1964–1971.
72. Suga, H., Schmid, V., and Gehring, W.J. (2008). Evolution and functional diversity of jellyfish opsins. Curr. Biol. *18*, 51–55.
73. Leung, N.Y., and Montell, C. (2017). Unconventional roles of opsins. Annu. Rev. Cell Dev. Biol. *33*, 241–264.
74. Blackshaw, S., and Snyder, S.H. (1999). Encephalopsin: a novel mammalian extraretinal opsin discretely localized in the brain. J. Neurosci. *19*, 3681–3690.
75. Halford, S., Freedman, M.S., Bellingham, J., Inglis, S.L., Poopalasundaram, S., Soni, B.G., Foster, R.G., and Hunt, D.M. (2001). Characterization of a novel human opsin gene with wide tissue expression and identification of embedded and flanking genes on chromosome 1q43. Genomics *72*, 203–208.
76. Kumbalasiri, T., and Provencio, I. (2005). Melanopsin and other novel mammalian opsins. Exp. Eye Res. *81*, 368–375.
77. Sikka, G., Hussmann, G.P., Pandey, D., Cao, S., Hori, D., Park, J.T., Steppan, J., Kim, J.H., Barodka, V., Myers, A.C., et al. (2014). Melanopsin mediates light-dependent relaxation in blood vessels. Proc. Natl. Acad. Sci. USA. *111*, 17977–17982.
78. Tarttelin, E.E., Bellingham, J., Hankins, M.W., Foster, R.G., and Lucas, R.J. (2003). Neuropsin (Opn5): a novel opsin identified in mammalian neural tissue. FEBS Lett. *554*, 410–416.
79. White, J.H., Chiano, M., Wigglesworth, M., Geske, R., Riley, J., White, N., Hall, S., Zhu, G., Maurio, F., Savage, T., et al.; GAIN investigators (2008). Identification of a novel asthma susceptibility gene on chromosome 1qter and its functional evaluation. Hum. Mol. Genet. *17*, 1890–1903.
80. Sukumaran, S.K., Lewandowski, B.C., Qin, Y., Kotha, R., Bachmanov, A.A., and Margolskee, R.F. (2017). Whole transcriptome profiling of taste bud cells. Sci. Rep. *7*, 7595.
81. Ren, W., Aihara, E., Lei, W., Gheewala, N., Uchiyama, H., Margolskee, R.F., Iwatsuki, K., and Jiang, P. (2017). Transcriptome analyses of taste organoids reveal multiple pathways involved in taste cell generation. Sci. Rep. *7*, 4004.
82. Vasiliauskas, D., Mazzoni, E.O., Sprecher, S.G., Brodetskiy, K., Johnston, R.J., Jr., Lidder, P., Vogt, N., Celik, A., and Desplan, C. (2011). Feedback from rhodopsin controls rhodopsin exclusion in *Drosophila* photoreceptors. Nature *479*, 108–112.
83. Yamaguchi, S., Wolf, R., Desplan, C., and Heisenberg, M. (2008). Motion vision is independent of color in *Drosophila*. Proc. Natl. Acad. Sci. USA *105*, 4910–4915.
84. Fischler, W., Kong, P., Marella, S., and Scott, K. (2007). The detection of carbonation by the *Drosophila* gustatory system. Nature *448*, 1054–1057.
85. Bischof, J., Maeda, R.K., Hediger, M., Karch, F., and Basler, K. (2007). An optimized transgenesis system for *Drosophila* using germ-line-specific phiC31 integrases. Proc. Natl. Acad. Sci. USA *104*, 3312–3317.
86. Sterling, T., and Irwin, J.J. (2015). ZINC 15—ligand discovery for everyone. J. Chem. Inf. Model. *55*, 2324–2337.
87. Dagan-Wiener, A., Di Pizio, A., Nissim, I., Bahia, M.S., Dubovski, N., Margulis, E., and Niv, M.Y. (2019). BitterDB: taste ligands and receptors database in 2019. Nucleic Acids Res. *47* (D1), D1179–D1185.
88. Wes, P.D., Xu, X.-Z.S., Li, H.-S., Chien, F., Doberstein, S.K., and Montell, C. (1999). Termination of phototransduction requires binding of the NINAC myosin III and the PDZ protein INAD. Nat. Neurosci. *2*, 447–453.

STAR★METHODS

KEY RESOURCES TABLE

REAGENT or RESOURCE	SOURCE	IDENTIFIER
Antibodies		
anti-GFP antibody (chicken)	Thermo Fisher Scientific	Cat#A10262; RRID: AB_2534023
anti-DsRed antibody (rabbit)	Clontech Laboratories, Inc.	Cat#632496; RRID: AB_10013483
anti-FLAG antibody (rabbit)	Sigma-Aldrich	Cat#F7425; RRID: AB_439687
Goat anti-chicken, Alexa488	Thermo Fisher Scientific	Cat#A11039; RRID: AB_142924
Goat anti-rabbit, Alexa488	Thermo Fisher Scientific	Cat#A11008; RRID: AB_143165
Goat anti-rabbit, Alexa568	Thermo Fisher Scientific	Cat#A11036; RRID: AB_10563566
Chemicals, Peptides, and Recombinant Proteins		
Sulforhodamine B	Sigma-Aldrich	Cat#230162
Brilliant Blue FCF	Wako Chemical	Cat#027-12842
Sucrose	Sigma-Aldrich	Cat#S0389
Aristolochic acid	Sigma-Aldrich	Cat#A9451
Piperonyl acetate	Sigma-Aldrich	Cat#W291218
Dry yeast	Genesee Scientific	Cat#62-103
D-(+)-glucose	Sigma-Aldrich	Cat#G8270
Rice powder	United Foodstuff Company	N/A
Agar	BD Diagnostics	Cat#214010
Cholesterol	Sigma-Aldrich	Cat#C8667
Methyl 4-hydroxybenzoate	Sigma-Aldrich	Cat#H5501
Propionic acid	Sigma-Aldrich	Cat#81910
Critical Commercial Assays		
BrightGlo reagent	Promega	Cat#E2610
Experimental Models: Cell Lines		
Human: HEK293T (HTLA)	Laboratory of Bryan Roth	N/A
Experimental Models: Organisms/Strains		
Drosophila: w^{1118}	Bloomington *Drosophila* Stock Center	Cat#BL5905
Drosophila: $ninaE^{I17}$	Bloomington *Drosophila* Stock Center	Cat#BL5701
Drosophila: $ninaE^{Df}$ [Df(3R)BSC636]	Bloomington *Drosophila* Stock Center	Cat#BL25726
Drosophila: $rh4^{Df}$ [Df(3L)Exel9003]	Bloomington *Drosophila* Stock Center	Cat#BL7936
Drosophila: $rh7^{Df}$ [Df(3L)BSC730]	Bloomington *Drosophila* Stock Center	Cat#BL26828
Drosophila: *rh1* RNAi	Bloomington *Drosophila* Stock Center	Cat#BL31647
Drosophila: *rh4* RNAi	Bloomington *Drosophila* Stock Center	Cat#BL77159
Drosophila: *rh7* RNAi	Bloomington *Drosophila* Stock Center	Cat#BL62176
Drosophila: $tubP\text{-}GAL80^{ts}$	Bloomington *Drosophila* Stock Center	Cat#BL7018
Drosophila: *rh1-GAL4*	Bloomington *Drosophila* Stock Center	Cat#BL68385
Drosophila: *rh4-GAL4*	Bloomington *Drosophila* Stock Center	Cat#BL8627
Drosophila: $G_{\alpha q}{}^{1}$ or $G_{\alpha q}49B^{1}$	Bloomington *Drosophila* Stock Center	Cat#BL42257
Drosophila: $G_{\alpha q}{}^{Df}$ [Df(2R)$G_{\alpha q}$1.3]	Bloomington *Drosophila* Stock Center	Cat#BL44611
Drosophila: $norpA^{36}$ or $norpA^{P24}$	Bloomington *Drosophila* Stock Center	Cat#BL9048
Drosophila: $norpA^{Df}$ [Df(1)BSC723]	Bloomington *Drosophila* Stock Center	Cat#BL26575
Drosophila: $ninaD^{1}$	Bloomington *Drosophila* Stock Center	Cat#BL42244
Drosophila: 15X*UAS-IVS-mCD8::GFP*	Bloomington *Drosophila* Stock Center	Cat#BL32193
Drosophila: *UAS-mCD8::dsRed*	Bloomington *Drosophila* Stock Center	Cat#BL27398
Drosophila: *40XUAS-IVS-mCD8::GFP*	Bloomington *Drosophila* Stock Center	Cat#BL32195
Drosophila: *Gr5a-GAL4*	Bloomington *Drosophila* Stock Center	Cat#BL57592

(*Continued on next page*)

Continued

REAGENT or RESOURCE	SOURCE	IDENTIFIER
Drosophila: *rh4*^{1}	[82]	N/A
Drosophila: *rh5*^{2}	[83]	N/A
Drosophila: *rh6*^{1}	*Drosophila* Genomics and Genetic Resources (Kyoto Stock Center)	Cat#109600
Drosophila: *UAS-rh1*	[82]	N/A
Drosophila: *UAS-rh4*	[82]	N/A
Drosophila: *Gr5a-I-GFP*	[84]	N/A
Drosophila: *Gr66-I-GFP*	[84]	N/A
Drosophila: *UAS-trpA1-C*	[45]	N/A
Drosophila: *UAS-trpA1-D*	[45]	N/A
Drosophila: *rh2*^{1}	Laboratory of Craig Montell	N/A
Drosophila: *rh3*^{2}	Laboratory of Craig Montell	N/A
Drosophila: *rh4*^{LexA}	This paper	N/A
Drosophila: *rh7*^{1}	Bloomington *Drosophila* Stock Center	Cat#BL76022
Drosophila: *Gr66a*^{ex83}	Bloomington *Drosophila* Stock Center	Cat#BL25027
Drosophila: *UAS-rh7*	Bloomington *Drosophila* Stock Center	Cat#BL76029
Drosophila: *trpA1*^{1}	Bloomington *Drosophila* Stock Center	Cat#BL26504
Drosophila: *trpA1-AB*^{GAL4}	Bloomington *Drosophila* Stock Center	Cat#BL67131
Drosophila: *trpA1-CD*^{GAL4}	Bloomington *Drosophila* Stock Center	Cat#BL67134
Drosophila: *Gr66a-GAL4*	Bloomington *Drosophila* Stock Center	Cat#BL28801
Drosophila: *UAS-rh1*^{K319R}	This paper	N/A
Oligonucleotides		
Rh1 RT-qPCR primer sequences: Forward CTTGTCCACCACCGATCCA Reverse TGACGCAGCCAGTAACCAAA	This paper	N/A
Rh4 RT-qPCR primer sequences: Forward TCACCAAGGCGGTGATAATG Reverse CGAAAGATAGTCGAAGGAGCAG	This paper	N/A
Rh7 RT-qPCR primer sequences: Forward GGCAATGTAGCTCAGGTCGT Reverse CGCTGTGAATGTAGGCAAGG	This paper	N/A
Alpha-tubulin RT-qPCR primer sequences: Forward TGTCGCGTGTGAAACACTTC Reverse AGCAGGCGTTTCCAATCTG	This paper	N/A
Recombinant DNA		
pUAST-attB	[85]	N/A
pCS3-MT	Laboratory of Dave Turner	Addgene Plasmid #2296
trpA1-C cDNA	This paper	FlyBase: FBtr0331824
trpA1-D cDNA	This paper	FlyBase: FBtr0331823
empty Tango vector (obtained from human OPN3: OPN3-Tango)	[31]	Addgene Plasmid #66459; RRID: Addgene_66459
Drosophila Rh7 (codon optimized): Rh7-Tango	This paper	N/A
Drosophila Rh1 (codon optimized): Rh1-Tango	This paper	N/A
Drosophila Rh7-Rh1-Rh7 (codon optimized): Rh7-Rh1-Rh7 Tango	This paper	N/A
Drosophila Rh4 (codon optimized): Rh4-Tango	This paper	N/A
Drosophila Rh7-Rh4-Rh7 (codon optimized): Rh7-Rh4-Rh7 Tango	This paper	N/A
Other		
Glass capillaries	World Precision Instruments	Cat#1B150F-3

LEAD CONTACT AND MATERIALS AVAILABILITY

All unique/stable reagents generated in this study are available from the Lead Contact without restriction. Further information and requests for resources and reagents should be directed to and will be fulfilled by the Lead Contact, Craig Montell (cmontell@ucsb.edu).

EXPERIMENTAL MODEL AND SUBJECT DETAILS

Fly stocks

Genotypes of the fruit fly *Drosophila melanogaster* used in this study are listed in the Key Resources Table. The following lines were obtained from the Bloomington *Drosophila* Stock Center: w^{1118} (5905), $ninaE^{I17}$ (5701; referred to here as $rh1^{I17}$), $ninaE^{Df}$ [Df(3R) BSC636] (25726), $rh4^{Df}$ [Df(3L)Exel9003] (7936), $rh7^{Df}$ [Df(3L)BSC730] (26828), *rh1* RNAi (31647), *rh4* RNAi (77159), *rh7* RNAi (62176), $tubP\text{-}GAL80^{ts}$ (7018), *rh1-GAL4* (68385), *rh4-GAL4* (8627), $G_{\alpha q}{}^{1}$ or $G_{\alpha q}49B^{1}$ (42257), $G_{\alpha q}{}^{Df}$ [Df(2R)$G_{\alpha q}$1.3] (44611), $norpA^{36}$ or $norpA^{P24}$ (9048), $norpA^{Df}$ [Df(1)BSC723] (26575), $ninaD^{1}$ (42244), 15X*UAS-IVS-mCD8*::*GFP* (32193), *UAS-mCD8*::*dsRed* (27398), *40XUAS-IVS-mCD8*::*GFP* (32195), and *Gr5a-GAL4* (57592). The following lines were provided by the indicated investigators: $rh4^{1}$, $rh5^{2}$, $rh6^{1}$, *UAS-rh1*, and *UAS-rh4* (C. Desplan), *Gr5a-I-GFP* and *Gr66-I-GFP* (K. Scott), *Gr66a-GAL4* (H. Amrein) *UAS-trpA1-C* and *UAS-trpA1-D* (W.D. Tracey). The following lines were created in our laboratory and those that are available from the Bloomington *Drosophila* Stock Center are indicated with stock numbers: $rh2^{1}$, $rh3^{2}$, $rh4^{LexA}$, $rh7^{1}$ (76022), $Gr66a^{ex83}$ (25027), $Gr33a^{GAL4}$ (31425), *UAS-rh7* (76029), $trpA1^{1}$ (26504), $trpA1\text{-}AB^{GAL4}$ (67131), $trpA1\text{-}CD^{GAL4}$ (67134), *Gr66a-GAL4* (28801), and $UAS\text{-}rh1^{K319R}$.

Fly husbandry

Flies were raised in vials or bottles containing standard cornmeal-yeast media at 25°C in a humidified chamber under 12 h light/12 h dark cycles unless indicated otherwise. All mutant lines were outcrossed into the background of the control flies (w^{1118}) for five generations. Crosses for the behavior experiments were performed by placing 20–30 virgin females and 20–30 males in bottles. Other crosses were performed by placing 5–10 virgin females and 5–10 males in vials. Both females and males were used in all experiments and were selected randomly.

For behavior experiments (Figures 1, 2, 3, 4, 5, 6, 7, S1, S2, S3, and S4), 50 randomly selected flies were collected into vials one day post-eclosion, group housed, and aged until 5–7 days old. Flies were starved in 1% agarose for 18–20 h in a humidified chamber prior to the experiment. Experiments were performed 4–6 h after onset of light. For tip recording experiments (Figures 1, 2, 3, 4, 5, 6, 7, S1, S2, S4, and S7), flies were collected into vials one day post-eclosion, group housed, and aged until 7–10 days old. For ERG experiments (Figures 3 and S3), flies were collected into vials one day post-eclosion, group housed, and aged until 5–7 days old. For carotenoid-deprived flies (Figures 3 and S3), the flies were allowed to mate on carotenoid-deficient food bottles for five days. To raise cartenoid-deficient flies, 50 randomly selected flies one day post-eclosion were collected into vials containing carotenoid-deficient food. Flies were transferred to fresh carotenoid-deficient food vials every three to four days and aged for the experiments. Flies used for immunostaining and cDNA sample preparation (Figures 4, 7, S4, and S7) were collected into vials one day post-eclosion, group housed, and aged until 5–7 days old.

Cell lines

The modified HEK293T cell line (HTLA) was obtained from the Bryan Roth laboratory. This cell line was maintained in DMEM with 10% fetal bovine serum (Thermo Fisher Scientific) and 1% Pen-Strep (Thermo Fisher Scientific) at 37°C, 80% humidity, and 5% CO_2.

METHOD DETAILS

Generating *UAS-rh1*^{K319R}

To create *UAS-rh1*^{K319R} flies, we changed the codon for residue 319 from AAA to CGA, thereby resulting in a lysine to arginine substitution. To introduce this mutation in the *rh1* (*ninaE*) coding region, we first amplified the wild-type cDNA from w^{1118} using the following primer pair:

5′-AGGGAATTGGGAATTCCAACATGGAGAGCTTTGCAGTAGC-3′ and 5′- ACAAAGATCCTCTAGATTATGCCTTGGACTCGGCC-3′. We then generated the nucleotide changes in codon 319 by amplifying the cDNA using the following primer pair: 5′-CATTTGGG GAGCTTGCTTCGCCCGATCGGCCGCCTGCTAC-3′ and 5′-CGAAGCAAGCTCCCCAAATGGTATTCAGTG-3′. We subcloned this product using In-Fusion (Clontech) between the EcoRI/XbaI sites of the pUAST-attB vector and injected the construct into the attP40 strain (BestGene).

Two-way choice feeding assays

Two-way choice feeding assays were performed as previously described [15] with slight modifications. 35–50 flies (aged to 5–7 days) per assay were starved in 1% agarose (Thermo Fisher Scientific) for 18–20 h in a humidified chamber. The fly genotypes in Figures 1B and 6A were blinded to the experimenter. Flies were tested in 72-well plates (Nunc) that contained tastant/dye mixtures, and allowed to feed for 3 h in the dark, unless indicated otherwise. The tastant/dye mixtures were added to low melting point agarose (Thermo Fisher Scientific) to avoid overheating of bitter compounds.

The preference index (PI) was calculated according to the following equation: $(N_{red} - N_{blue})/(N_{red} + N_{purple} + N_{blue})$. We determined the concentrations of the red (Sulforhodamine B; Sigma-Aldrich) and blue (Brilliant Blue FCF; Wako Chemical) food dyes that had no significant effect on food selection by assaying the preference of control flies to each dye with 2 mM sucrose (Figures S1A and S1B). Once the concentrations were established that lead to indifference between the two food colorings, we used red dye for sucrose-only food and blue dye for food with sucrose plus bitter compound. A PI = 1.0 and −1.0 indicates complete preference for food with sucrose-only and sucrose plus bitter compound, respectively. A PI = 0 indicated no preference for either food. Trials in which < 70% of the flies participated were discarded.

Extracellular tip recordings

Extracellular tip recordings were performed as previously described with slight modifications [16]. Flies aged 7–10 days were used for recordings. The fly genotypes in Figures 1D and 6C were blinded to the experimenter. Aristolochic acid was dissolved in 1 mM KCl, which served as the electrolyte, and backfilled into recording electrodes (World Precision Instruments, 1B150F-3) with 20 μm openings (Sutter Instrument, P-97 puller). Tastant-induced signals were amplified and digitalized with an IDAC-4 data acquisition device and Autospike software (Syntech). Spike sorting was used to identify spike amplitudes that correspond to the action potentials of bitter-responsive neurons. Neuronal responses were quantified by counting the number of action potentials between 200–1,200 ms following contact with the stimulus.

Chemicals for feeding assays and tip recordings

The following compounds were purchased from Sigma-Aldrich: sucrose, aristolochic acid I sodium salt, and piperonyl acetate. The stock solution of aristolochic acid was dissolved in water up to 10 mM. The stock solution of piperonyl acetate was dissolved in ethanol up to 100 mM. The same amount of ethanol was added to the sucrose-only food and tastant solution to control for any behavior or electrophysiological effects of ethanol.

Cell culture and β-arrestin recruitment assay

Cell culture and the GPCR β-arrestin recruitment assay (TANGO) were performed as described [31] with minor modifications. The Rh7 coding sequence with an N-terminal FLAG tag was codon optimized and synthesized by IDT. The construct was cloned into the TANGO vector (Addgene) at the ClaI site (FLAG::Rh7). The HTLA cells (modified HEK293T cells; a gift from the Bryan Roth laboratory) were transfected in a 6-well format with Lipofectamine 2000 (Thermo Fisher Scientific) according to the manufacturer's instructions. 6–8 h post transfection we split the cells 1:3 and replaced the media with DMEM + 2.5% fetal bovine serum (Thermo Fisher Scientific). We allowed the cells to grow for 48 h before splitting the cells into poly-L-lysine-coated 96-well clear, flat bottom white polystyrene plates (Corning) in serum-free media. The next day drug solutions diluted in TANGO assay buffer (20 mM HEPES, 1x HBSS, pH 7.40) were added to the cells. After 4 h, the medium and drug solutions were removed and replaced with 40 μL per well of BrightGlo reagent (Promega) diluted 20-fold with TANGO assay buffer. We incubated the plates for 20 min at room temperature in the dark before measuring luminescence with a plate reader (Molecular Devices, iD3). The normalized response is calculated using following formula: RLU (relative luminescence units) = test compound RLU – average vehicle control RLU.

Aristolochic acid analogs

To identify analogs of aristolochic acid, we screened ZINC, a database of millions of purchasable compounds [86], and BitterDB, a database of bitter compounds [87]. We performed a similarity search through ZINC and BitterDB by applying a Tanimoto coefficient cutoff of 0.5 and filtered out chromophore-based derivatives in order to explore different chemical scaffolds. The remaining compounds were submitted to a 3D shape similarity screening with Phase (Schrödinger Release 2018-1, Phase, Schrödinger, LLC, New York, NY, 2018) using the aristolochic acid structure as the query. The list was narrowed to 11 compounds according to the ranking score and by visual inspection. We selected to test piperonyl acetate based on commercial availability and solubility.

Homology modeling of Rh7

We modeled the 3D structure of the Rh7 transmembrane domains by GPCR-I-TASSER, a fragment-based method in which fragments are excised from GPCR template structures and reassembled based on threading alignments [36]. The crystal structures that mostly contributed to the modeling were the human (PDB: 4ZWJ), bovine (PDB: 1GZM), and squid (PDB: 2Z73) rhodopsins. We predicted ligand binding modes of aristolochic acid and piperonyl acetate to Rh7 using Induced Fit Docking (Schrödinger Release 2018-1, Induced Fit Docking protocol; Glide, Schrödinger, LLC, New York, NY, 2018; Prime, Schrödinger, LLC, New York, NY, 2018). The grid box was centroid to the retinal coordinates in bovine rhodopsin. The docking was performed using the Standard Precision (SP) mode of Glide (Table S2).

Quantitative PCR

To detect expression of *opsin* mRNAs in the head and labellum by reverse transcription PCR (RT-PCR) and quantitative PCR (RT-qPCR), we isolated RNA from 5 heads without labella and 25 labella using TRIzol (Thermo Fisher Scientific). We prepared cDNA using SuperScript III Reverse Transcriptase (Thermo Fisher Scientific) with oligodT primers. For RT-PCR, we amplified for

40 cycles using Phusion DNA polymerase (New England BioLabs) and for RT-qPCR, we amplified for 50 cycles using the LightCycler 480 SYBR Green I Master Mix (Roche). *rh1*, 5′- CTTGTCCACCACCGATCCA-3′ and 5′-TGACGCAGCCAGTAACCAAA-3′ (103 bp); *rh4*, 5′- TCACCAAGGCGGTGATAATG-3′ and 5′-CGAAAGATAGTCGAAGGAGCAG-3′ (134 bp); *rh7*, 5′-GGCAATGTAGCTCAG GTCGT-3′ and 5′-CGCTGTGAATGTAGGCAAGG-3′ (127 bp); and *α-tubulin*, 5′-TGTCGCGTGTGAAACACTTC-3′ and 5′-AGCAG GCGTTTCCAATCTG-3′ (96 bp).

Immunostaining

Labella: Dissected labella from 5- to7-day-old adult flies were fixed in 4% paraformaldehyde in PBST (PBS + 0.5% Triton X-100) for 30 min at room temperature. Samples were washed in PBST (10 min, 3 times) and blocked with 5% normal goat serum (MP Biomedicals) in PBST (block buffer) for 30 min at room temperature, followed by incubation with primary antibodies in blocking buffer overnight 10°C. The samples were washed with PBST (10 min, 3 times) and incubated with the secondary antibodies in blocking buffer overnight at 4°C in the dark. After a final PBST wash (10 min, 3 times), the samples were mounted using Vectashield (Vector Laboratory, H-1000) and a coverslip was secured with nail polish. The samples were imaged using a Zeiss LSM 700 confocal laser scanning microscope using a 20x/0.8 Plan-Apochromat DIC objective. The images were processed using Zen software and ImageJ. The following primary and secondary antibodies were used at the indicated dilutions: chicken anti-GFP (1:200; Thermo Fisher Scientific), rabbit anti-DsRed (1:500; Clontech), AlexaFluor 488 goat anti-chicken IgG (1:1000; Thermo Fisher Scientific), AlexaFluor 568 goat anti-rabbit IgG (1:1000; Thermo Fisher Scientific).

Cell culture: Cells were plated at a density of 40,000 cells per well onto 7 mm coverslips (Warner Instruments) in 24-well plates 2–4 h before fixation. For permeabilized cells, the procedure was as stated above. For non-permeabilized cells, Triton X-100 was omitted. The samples were mounted using Vectashield with DAPI (Vector Laboratory, H-1500). The following primary and secondary antibodies were used at the indicated dilutions: rabbit anti-FLAG (1:500; Sigma-Aldrich), AlexaFluor 488 goat anti-rabbit IgG (1:1000; Thermo Fisher Scientific).

Recipe for carotenoid-deficient food

The carotenoid-deficient food was comprised of the following ingredients: 40 mg/mL dry yeast (Genesee Scientific), 40 mg/mL D-(+)-glucose (Sigma-Aldrich), 48 mg/mL rice powder (United Foodstuff Company), 8 mg/mL agar (BD Diagnostics), 0.24 mg/mL cholesterol (Sigma-Aldrich), 3.6 mg/mL methyl 4-hydroxybenzoate (Sigma-Aldrich), and 0.32% (v/v) propionic acid (Sigma-Aldrich).

Electroretinogram recordings

Electroretinogram recordings were performed as previously described [88] with slight modifications. Briefly, two glass electrodes filled with Ringer's solution were inserted into small drops of electrode cream placed on the surfaces of the compound eye and the thorax. Flies were exposed to 10 s of orange light (Klinger Educational Products, 580 nm filter). Light-induced signals were amplified using an IE-210 amplifier (Warner Instruments) and the data were acquired with a Powerlab 4/30 device and LabChart 6 software (AD Instruments).

Two-electrode voltage clamp recordings

We subcloned the *trpA1-C* and *trpA1-D* cDNAs (referred to as *trpA1-RH* and *trpA1-RG* in FlyBase) into the NotI site of the pCS2-MT vector (Addgene), and synthesized cRNAs using the mMESSAGE mMACHINE SP6 transcription kit (Thermo Fisher Scientific). We surgically removed oocytes from *Xenopus laevis* and maintained them in OR3 medium (50% (v/v) L-15 Leibovitz's medium (Thermo Fisher Scientific), 15 mM HEPES, 0.1 mg/mL Gentamicin (Sigma-Aldrich), 0.2% (v/v) Fungizone (Sigma-Aldrich), 100 μg/mL penicillin/streptomycin, pH 7.5) for 24 h at 18°C before injecting them with ~40 ng cRNA using a micro-injector (Nanoject, Drummond Scientific). We allowed the injected oocytes to recover for 48 h in OR3 medium at 18°C before performing the recordings. We held the oocytes at −40 mV and recorded the whole-cell currents before and after chemical perfusion. We diluted the chemicals in Ca^{2+}- and Mg^{2+}-free ND96 buffer (96 mM NaCl, 2 mM KCl, 5 mM HEPES, pH 7.5) to minimize precipitation of aristolochic acid.

QUANTIFICATION AND STATISTICAL ANALYSIS

All error bars represent standard error of the mean (SEM). The number of times each experiment was repeated (n) are indicated in the figure legends. For the two-way choice assays each ''n'' represents a single test performed with 35–50 animals. Each ''n'' for the tip recordings represents an analysis of a single, independent fly. Each ''n'' for the ERGs represents an analysis of a single, independent fly. For RT-qPCR experiments, the data are represented as the mean of three independent experiments. For the β-arrestin recruitment assay, the data are represented as the mean of four independent experiments. All graphs were generated using Prism 7 (Graphpad).

For behavior and electrophysiology (tip recording) experiments, we estimated the sample size using preliminary data obtained with control (w^{1118}) and $rh1^{l17}$ mutant flies ($ninaE^{l17}$) flies with an n = 5. We set the significance level, $\alpha = 0.05$ and power, $1\text{-}\beta = 0.9$. For sample size calculations, we assumed that the preliminary data follow a normal distribution. The power calculator estimated n = 8 for the two-way choice assay and n = 12 for the tip recordings.

We tested each dataset for normality using the Shapiro-Wilk test. For parametric tests, we used the unpaired Student's t test and the one-way ANOVA with Tukey's multiple comparisons test. For non-parametric tests, we used the Mann-Whitney test and the Kruskal-Wallis test with Dunn's multiple comparisons test. The statistical test used are indicated in the figure legends. Statistical tests were performed using Prism 7 (Graphpad). Asterisks indicate statistical significance, where *$p < 0.05$, **$p < 0.01$, and ***$p < 0.001$.

DATA AND CODE AVAILABILITY

This study did not generate/analyze datasets or code.